

University of Missouri, St. Louis

IRL @ UMSL

---

Theses

UMSL Graduate Works

---


7-6-2017

## Rational Drug Design Directed at Blocking the Initial Signaling Events in Lipopolysaccharide-Induced Sepsis.

Christopher A. Tipton

*University of Missouri - St. Louis*, cattk8@mail.umsl.edu

Follow this and additional works at: <https://irl.umsl.edu/thesis>

 Part of the [Biochemistry Commons](#), [Biotechnology Commons](#), [Immunoprophylaxis and Therapy Commons](#), [Medicinal-Pharmaceutical Chemistry Commons](#), [Molecular Biology Commons](#), and the [Organic Chemistry Commons](#)

---

### Recommended Citation

Tipton, Christopher A., "Rational Drug Design Directed at Blocking the Initial Signaling Events in Lipopolysaccharide-Induced Sepsis." (2017). *Theses*. 305.  
<https://irl.umsl.edu/thesis/305>

This Thesis is brought to you for free and open access by the UMSL Graduate Works at IRL @ UMSL. It has been accepted for inclusion in Theses by an authorized administrator of IRL @ UMSL. For more information, please contact [marvinh@umsl.edu](mailto:marvinh@umsl.edu).

**Rational Drug Design Directed at Blocking  
the Initial Signaling Events in  
Lipopolysaccharide-Induced Sepsis.**

Christopher A. Tipton CCEMT-P NR-P  
Student Education/Degrees  
B.S. Agriculture, University of Missouri-Columbia, 2007  
Nationally Registered Paramedic, 2009  
Critical Care, University of Maryland-Baltimore County, 2011

A Thesis Submitted to The Graduate School at the University  
of Missouri-St. Louis  
in partial fulfillment of the requirements for the degree  
Master of Science in Biochemistry & Biotechnology

August  
2017  
**Month and Year of graduation**

Advisory Committee

Michael Nichols, Ph.D.  
Chairperson

Christopher Spilling, Ph.D.  
Co-Chair

James Bashkin D. Phil.

Keith Stine Ph.D.

# Table of Contents

- i. List of Abbreviations
- ii. Abstract
- I. Introduction
  - 1. Immunopathogenesis
  - 2. Endotoxin
  - 3. Sepsis
  - 4. Current Interventions for Sepsis
- II. Background
  - A. Structure of LPS**
    - 1. The Core Region
    - 2. The O-antigen Region
    - 3. Lipid A
  - B. The LPS Receptor Complex**
    - 1. LBP & CD14
    - 2. TLR4-MD-2 Complex
    - 3. Signal Transduction Pathway & Mediators
    - 4. Alternate TRIF-dependent Pathway
    - 5. TNF $\alpha$
    - 6. Coagulation Cascade
  - C. Lipid A Analogues**
    - 1. Monosaccharide Mimetics
    - 2. Antagonizing LPS-Induced Dimerization
  - D. Phosphonates**
    - 1. Phosphono-sugar analogues
- III. Results & Discussion
  - 1. Development of Lipid X Mimetics
  - 2. Overall Synthesis
  - 3. Protecting Group Strategy
  - 4. Anomeric Hemiacetal Protection
  - 5. Synthesis of Lactone Derivatives
  - 6. Chemistry of Horner-Emmons Reaction
  - 7. Biological Activity Assay
  - 8. Biological Activity
- IV. Conclusion & Future Directions
- V. Experimentals
- VI. References

This page intentionally left blank

## **i. Abbreviations**

2-Keto-3-Deoxyoctonic acid (**Kdo**); 3-O-desacyl-4'-Monophosphoryl Lipid A (**MPL**); Arterial Carbon Dioxide (**PaCO<sub>2</sub>**); Bacterial and Permeability-Increasing protein (**BPI**); Dimethyl Sulfoxide (**DMSO**); Disseminated Intravascular Coagulation (**DIC**); Endoplasmic Reticulum (**ER**); Enzyme-Linked Immunosorbent Assay (**ELISA**); Human Acute Monocytic Leukemia Cells (**THP-1**); Inhibitor of  $\kappa$ B (**I $\kappa$ B**); Inhibitor of  $\kappa$ B Kinase (**IKK**); Interleukin-1 Receptor-Associated Kinase 4 (**IRAK4**); Leucine-Rich Repeat Regions (**LRR**); Lipopolysaccharide (**LPS**); LPS Binding Protein (**LBP**); Membrane anchored CD14 (**mCD14**); Myeloid Differentiation primary response gene 88 (**MyD88**); Myeloid Differentiation protein-2 (**MD-2**); N-Methylmorpholine N-Oxide (**NMO**); Nitric Oxide (**NO**); Nuclear Factor  $\kappa$ B (**NF $\kappa$ B**); Pathogen-Associated Molecular Patterns (**PAMPs**); Pattern Recognition Receptors (**PRRs**); Soluble CD14 (**sCD14**); Sterile  $\alpha$  and HEAT-Armadillo Motif-containing protein (**SARM**); Systemic Inflammatory Response Syndrome (**SIRS**); Tetrapropylammonium Perruthenate (**TPAP**); TIR domain-containing adapter Inducing IFN- $\beta$  (**TRIF**); TIR domain-containing Adapter Protein (**TIRAP**); Toll Interleukin-1 Receptor (**TIR**); Toll-Like Receptor 4 (**TLR4**); Toll-Like Receptors (**TLR**); TRIF-Related Adapter Molecule (**TRAM**); Trimethylsilyl Bromide (**TMSBr**); Tumor Necrosis Factor  $\alpha$  (**TNF $\alpha$** )

## **ii. Abstract**

Systemic Inflammatory Response Syndrome (SIRS) is classified as an immune system response to an infectious state. If left untreated, SIRS leads to sepsis, septic shock, end-organ dysfunction, and death. As a patient progresses through these stages, associations of acute respiratory distress, disseminated intravascular coagulation, and acute renal failure persist, resulting in millions of deaths annually. Lipopolysaccharide (LPS), a bacterial endotoxin, is

released into the blood stream, triggering SIRS. LPS is found in the outer cell-wall of Gram-negative bacteria and is responsible for initiation of a devastating cytokine storm. One of the regions of LPS, lipid A, is a polyacylated glucosamine disaccharide that is primarily responsible for the pathological response of the immune system. LPS interacts with a plasma-LPS binding protein (LBP) via the lipid A region. LPS-LBP signals the CD14 receptor found on phagocytes and Toll-like receptors (TLR4), which results in a signaling pathway for inflammatory molecules like cytokines, TNF $\alpha$ , among numerous others. Antibiotic treatments alone prove insufficient; with numerous research data indicating increased bacterial resistance.

It has been demonstrated that compounds resembling the lipid A region can act as antagonist to LPS signaling and would de-activate the inflammatory cascade. Blocking this cascade of events, in conjunction with other known sepsis treatments, would prove beneficial to patient prognoses. Lipid A analogues have been developed which are antagonists of LPS signaling and do not activate the inflammatory cascade. The most interesting antagonists are the monosaccharides, which demonstrate that the glucosamine nitrogen can be replaced by oxygen and acyl groups can be replaced by more robust ethers.

# **I. Introduction**

## **1. Immunopathogenesis**

Our innate immunity has evolved into a complex system that elicits a response to pathogenic microbes to achieve a survival advantage. The immune response attempts to localize the infection and repair the damaged tissue. This is achieved by activation of circulating and fixed phagocytic cells and the production of pro-inflammatory and anti-inflammatory mediators. The balance between these mediators facilitates tissue repair, while simultaneously keeping the infection from spreading. When the inflammatory response extends beyond the infected tissues and becomes generalized, this balance is lost. The process to control infection then becomes uncontrolled and unregulated, leading to sepsis.

## **2. Endotoxin**

Near the turn of the 20<sup>th</sup> century, it was discovered that heat-killed *Vibrio cholerae* were intrinsically toxic as opposed to producing toxicity by secretion of a product. To

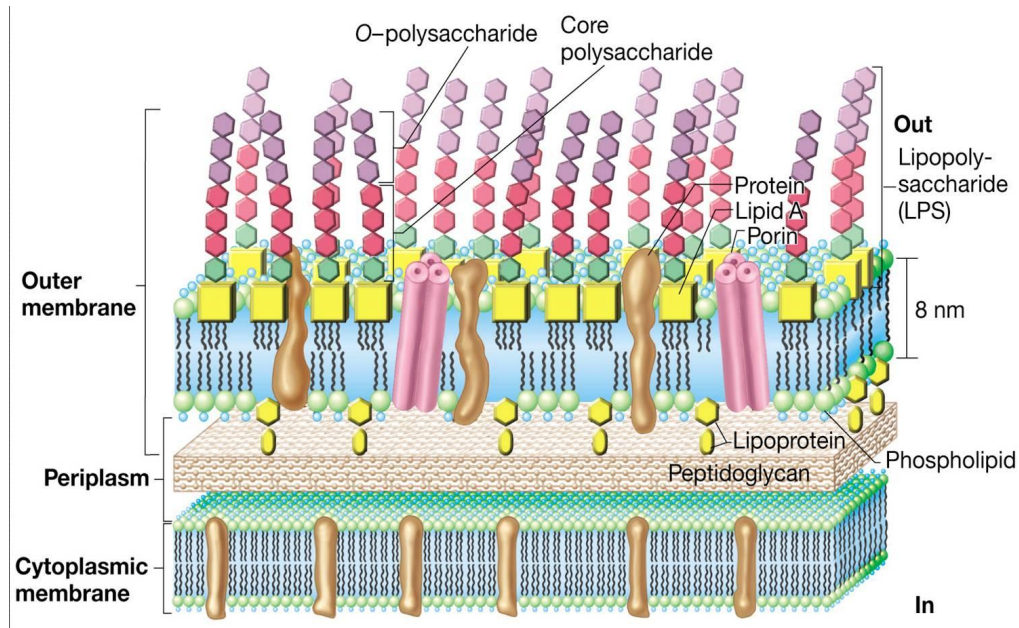


**Figure 1<sup>1</sup> | Cell-wall of Gram-negative Bacteria.**

Organization of lipopolysaccharide, lipid A, lipoprotein, porins, peptidoglycan and phospholipid. The outer membrane is an asymmetric bilayer. The outer-leaflet of the outer membrane is highly distinctive due to the presence of lipopolysaccharide. The cytosolic bilayer consists of conventional phosphoglycerides.

differentiate, toxicity from a secreted product became recognized as an exotoxin while the toxic components of bacteria themselves were termed endotoxins. After further characterizations, these heat-stable endotoxins became known as lipopolysaccharide (LPS) and are localized to the cell-wall of Gram-negative bacteria. Gram-negative bacteria feature peptidoglycan that is encapsulated by two distinct lipid membranes (Figure 1<sup>1</sup>). The cytosolic bilayer consists of conventional phosphoglycerides, whilst the outer membrane is profoundly distinctive. The outer membrane is an



asymmetric bilayer and LPS is the primary constituent of the outer leaflet, of which lipid A is an integral component.

Pyrogenic bacteria generate endotoxins that stimulate the release of inflammatory mediators, leading to fever and systemic effects of inflammation advancing to septicemia. LPS may be released from the membrane during bacterial growth or during treatment with antibiotics. Intriguingly, relatively low concentrations of LPS can act as an immune-modulator by inducing non-specific resistance to both bacterial and viral infections.<sup>2</sup>

### **3. Sepsis**

Sepsis is a highly complex, variable and multifactorial disease process caused by the over-exaggeration of the host's response to endotoxin.<sup>3</sup> Predominantly responsible for Gram-negative bacteremia are Enterobacteriaceae and *Pseudomonas*, although other microorganisms can induce a similar response. Clinicians consider Gram-negative bacteremia as an idiosyncratic ailment due to its distinct clinical manifestations, epidemiology, pathogenesis, and treatment. Therefore, a consensus of the progression through stages of the illness was adopted by physicians. To start, systemic inflammatory response syndrome (SIRS) is classified as an immune system response to an infectious state and is evident

with at least two of the following patient indicators: (1) temperature greater than 38° C or less than 36° C; (2) heart rate greater than 90 beats per min; (3) tachypnea, which is defined as a respiratory rate greater than 20 breaths per minute coupled with an arterial carbon dioxide (PaCO<sub>2</sub>) less than 32 mmHg; (4) an alteration of white blood cell counts of greater than 12,000 cells/mm<sup>3</sup>, less than 4,000 cells/mm<sup>3</sup>, or greater than 10% immature neutrophils.<sup>3</sup> Furthermore, severe sepsis is defined as illness complicated by hypoperfusion abnormalities like: lactic acidosis, oliguria, and/or mental status changes, eventually leading to hypotension. Septic shock is used to reference the illness when associated with

<b>Table 1. The 20 most expensive conditions treated in U.S. hospitals, all payers, 2013</b>					
<b>Rank</b>	<b>CCS principal diagnosis category</b>	<b>Aggregate hospital costs, \$ millions</b>	<b>National costs, %</b>	<b>Number of hospital stays, thousands</b>	<b>Hospital stays, %</b>
<b>1</b>	<b>Septicemia</b>	<b>23,663</b>	<b>6.2</b>	<b>1,297</b>	<b>3.6</b>
<b>2</b>	<b>Osteoarthritis</b>	<b>16,520</b>	<b>4.3</b>	<b>1,023</b>	<b>2.9</b>
<b>3</b>	<b>Liveborn</b>	<b>13,287</b>	<b>3.5</b>	<b>3,765</b>	<b>10.6</b>
<b>4</b>	<b>Device complications, implant or graft</b>	<b>12,431</b>	<b>3.3</b>	<b>632</b>	<b>1.8</b>
<b>5</b>	<b>Acute myocardial infarction</b>	<b>12,092</b>	<b>3.2</b>	<b>602</b>	<b>1.7</b>

**Table 1<sup>5</sup> | Epidemiology of Sepsis**  
 Abbreviation: CCS, Clinical Classifications Software  
 Sources include: Agency for Healthcare Research and Quality (AHRQ), Center for Delivery, Organization, and Markets, Healthcare Cost and Utilization Project (HCUP), National Inpatient Sample (NIS), 2013

hypotension that is not responsive to fluid resuscitation. If left untreated, SIRS leads to sepsis, severe sepsis, septic shock, end-organ dysfunction, and death. As a patient progresses through these stages, associations of acute respiratory distress, disseminated intravascular coagulation (DIC), and acute renal failure persist,<sup>3</sup> resulting in millions of deaths annually.<sup>4</sup> In fact, sepsis is the leading cause of death in noncoronary intensive care units and amounts to as much as \$24 billion in annual healthcare expenditures in the United States alone (**Table 1**<sup>5</sup>).<sup>6</sup>

#### **4. Current Interventions for Sepsis**

The treatment of Gram-negative bacteremia traditionally involves three basic principles. First is identification and management of primary sites of infection. Resolution of bacteremia may depend upon successful management of the loci of infection and rapid identification of microorganisms responsible by Gram staining and culture of inflammatory material such as blood, sputum, urine, cerebral spinal or synovial fluid, etc. Second, there is an ongoing assessment of physiological parameters with interventions to support vital organ perfusion. For instance, the presence of hypotension is first treated with fluid resuscitation to expand intravascular volume. Persistent hypotension is

treated with sympathomimetic amines including dopamine, dobutamine and isoproterenol. Levophed (norepinephrine) is an intense vasoconstrictor considered if the previous sympathomimetics are found ineffective. Third, the administration of intravenous antibiotic therapy appropriate for the spectrum of bacteria. However, this classical triad of treatments is not geared towards blocking the toxic effects of endotoxin, which are further exaggerated by bacterial lysis from antibiotic therapy. Consequently, antibiotics alone do not alleviate, but rather increase the toxic effects of LPS in the septicemic patient.<sup>7</sup> The ensuing fluid administration and sympathomimetic treatments are merely supportive measures aimed to combat subsequent hemodynamic compromise from the overzealous host response. Whilst these treatments are necessary, future sepsis treatments should be spearheaded towards treating immunopathogenesis, not its symptoms.

Clearly, the pathophysiology of sepsis is extraordinarily complex. Exacerbating this complexity, patients that are susceptible to infection have many other medical conditions that affect their immune responsiveness and contribute to mortality. A distinct combination of therapies with a patient that is neutropenic (low neutrophils in bloodstream)<sup>8</sup> may differ for adjunctive therapies in an

elderly patient with a perforated diverticulum (bulging sac on the colon wall).<sup>9</sup> Presumably, an intervention with a single agent at a single time point in the progression of sepsis is unlikely to be effective. Advancement in treatments of sepsis may depend upon disrupting underlying mechanisms of immunopathogenesis responsible for tissue damage.

Corticosteroids have been researched as a potential adjuvant therapy due to their ability to attenuate the inflammatory response. However, in phase 3 clinical trials mortality rates of patients receiving corticosteroid treatment and a placebo were similar.<sup>10,11</sup> Opioid receptor blockers such as naloxone demonstrated improved survival in animal studies, as did corticosteroids. Similarly, naloxone failed to show any significant difference in mortality rates in human trials.<sup>12</sup>

Neutralization of endotoxin could be an attractive treatment against Gram-negative bacteremia induced sepsis. Past studies in humans using antibodies to endotoxin by administering polyclonal antiserum raised against core polysaccharide and lipid A regions of LPS demonstrated significantly reduced mortality rates.<sup>13</sup> However, the associated cost of producing antiserum coupled with the potential for transmission of infection prevented the widespread use of this treatment.

An approach that would circumvent the complications of cost and transmission of infection could be the development of nontoxic lipid A analogues. In animal models, enhanced survival from Gram-negative bacteremia using lipid A analogues has been demonstrated.<sup>14</sup> An in-depth analysis of the initial events in LPS-signaling is essential to develop a rational therapy directed at blocking LPS-induced sepsis. Additionally, illuminating the structural components of LPS responsible for immunopathogenesis is vital to identify therapeutic targets.

## **II. Background**

### **A. *Structure of LPS***

Early attempts to elucidate the structure of LPS failed for many reasons. LPS is highly amphipathic and has an inherent tendency to aggregate through hydrophobic bonding or by crosslinking via ionic interactions. Mildly acidic conditions using trichloroacetic acid to extract and purify LPS was first performed by Boivin *et. al.* in the 1930s. However, LPS purified by the Boivin method was in effect a crude fraction containing many cell-wall contaminants. It was

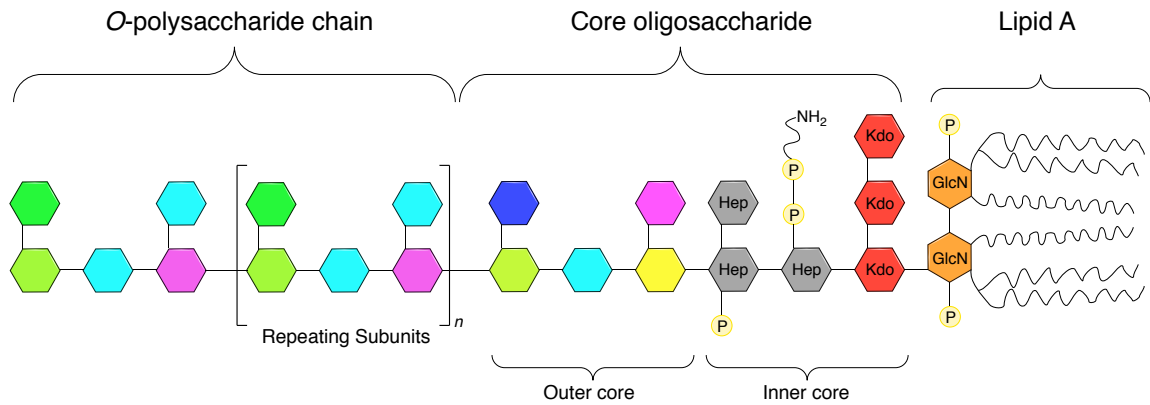


**Figure 2<sup>1</sup> | Structure of LPS.**

The three major regions of LPS are: O-polysaccharide, Core oligosaccharide, and lipid A. O-polysaccharide is highly variable, but the Core and lipid A regions are more conserved between *Bacteria*. The lipid A portion of LPS is responsible for endotoxicity. Hep, heptose; Kdo, 2-keto-3-deoxyoctonate; GlcN, glucosamine; P, phosphate.

not until later that Westphal and Luderitz *et. al.* developed an improved method for isolating endotoxin, which led to the LPS nomenclature.<sup>15</sup> Today, modern mass spectrometry with matrix-assisted laser desorption and electrospray ionization has been pivotal for characterizing intricate details of LPS between species.<sup>16</sup> Accordingly, LPS derived from all characterized Gram-negative bacteria are composed of three distinct regions, namely lipid A, core oligosaccharide and O-antigen repeats (**Figure 2<sup>1</sup>**). Lipid A contains a hydrophobic region that anchors LPS to the outer leaflet of the outer membrane. Distal to lipid A is a core oligosaccharide area consisting of sugar residues with multiple phosphoryl substituents, followed by a structurally diverse polymer

called *O*-antigen that is composed of repeat oligosaccharide units.<sup>16</sup> Both core oligosaccharide and *O*-antigen are displayed on the surface of Gram-negative bacterial cells. The remaining surface of the outer leaflet of the outer membrane is taken up by proteins, while the inner leaflet contains conventional phosphoglycerides, mostly phosphatidylethanolamine/glycerol and cardiolipin.<sup>16</sup>

### 1. The Core Region

The core region is more architecturally uniform than the outer *O*-antigenic region, exhibiting moderate interbacterial variability.<sup>17</sup> The inner core contains characteristic components heptose and 2-keto-3-deoxyoctonic acid (Kdo). Predominantly, the inner core contains two or more Kdo residues and two or three L-glycero-D-manno-heptose residues (Figure 3<sup>16</sup>). The Kdo residue is positioned at the reducing end of the inner core and is linked to C-

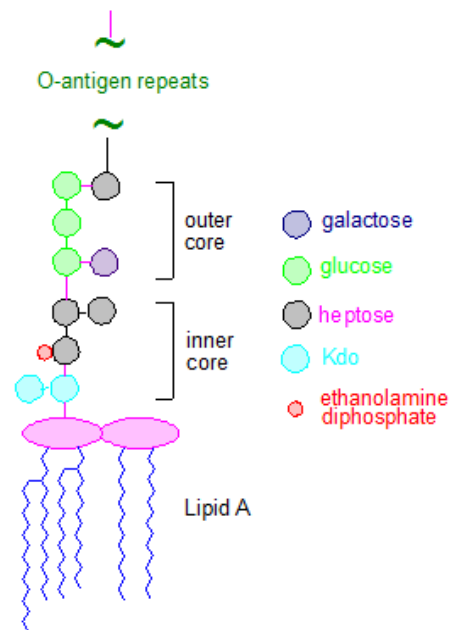


**Figure 3<sup>16</sup> | The Core region.**

The inner core usually consists of two Kdo and three L-glycero-D-manno-heptose residues. The outer core is composed of conventional sugars such as glucose and/or galactose.



6' of the two hexosamine (lipid A) residues. The L-glycerol-D-manno-heptose residues are located on the other side of the short oligosaccharide inner core chain. Both Kdo and L-glycerol-D-manno-heptose residues are unique to bacteria.<sup>18</sup> In contrast, the outer core region consists of commonly observed sugars and is more variable than the inner core. The outer core region is generally two or three residues long with one or more covalently bound polysaccharides as side chains<sup>19</sup> (**Figure 3**<sup>16</sup>).

## **2. The O-antigen region**

Attached at the terminal sugar of the core region, further extending extracellularly are repeating units of oligosaccharides comprising the O-antigen region. By position, it is the O-antigen region that encounters the hosts defense mechanisms during infection while also shielding the effects of antibiotic treatments. O-antigen also forms the basis of serotype classification of bacterial genera.<sup>20</sup> It consists of zero to as many as 40 repetitive oligosaccharide subunits, which in turn contain two to seven monosaccharide residues.<sup>20</sup> The inherent diversity of monosaccharides arising from alternative configurations, coupled with innumerable variability in glycosidic linkages, results in the O-antigen region being the most variable component of LPS, and unique

to individual bacterial strains. Significantly, when separated from the lipid A component of LPS, neither the O-antigen nor the core polysaccharide exhibit endotoxic activity.<sup>20</sup>

### 3. Lipid A

Lipid A is a distinct phosphoglycolipid and the fundamental backbone structure is highly conserved amongst bacteria (Figure 4<sup>21</sup>).<sup>22</sup> All contain D-gluco-configured pyranose hexosamine residues that are  $\beta$  (1 $\rightarrow$ 6) linked dimers.<sup>16</sup> Also, the disaccharide component consists of  $\alpha$ -glycosidic and non-glycosidic phosphoryl substituents located at C-1 and C-4'. The phosphorylated disaccharide backbone contains ester or amide linkages at positions O-2, O-3, O-2' and O-3' of (R)-3-hydroxy fatty acids, of which two are usually further acetylated.<sup>16</sup>

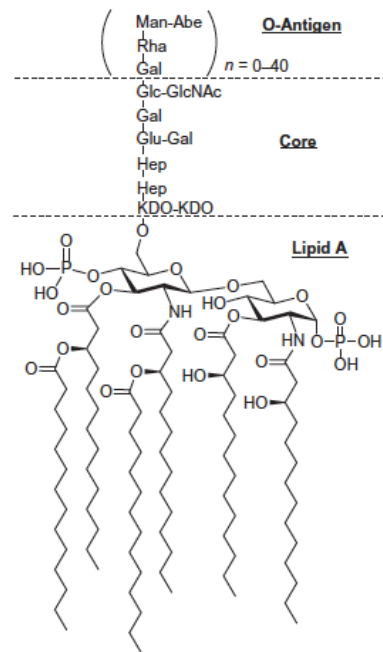


**Figure 4<sup>21</sup> | Lipid A**  
Lipid A functions as an anchor by binding LPS to peptidoglycan with fatty acid chains. Fatty acids widely recognized include: caporic (C<sub>6</sub>), lauric (C<sub>12</sub>), myristic (C<sub>14</sub>), palmitic (C<sub>16</sub>), and steric (C<sub>18</sub>) acids.

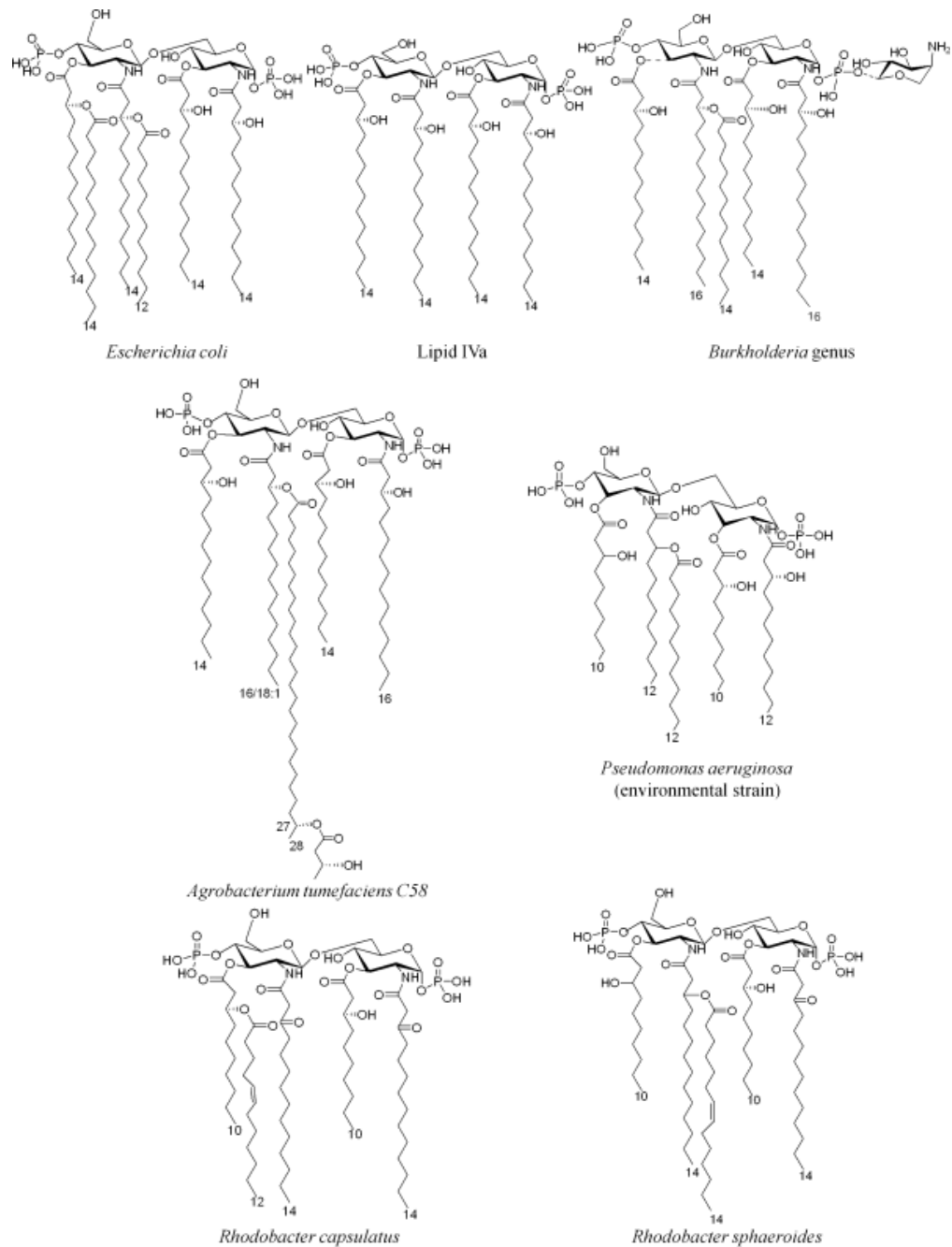


**Figure 5<sup>23</sup> | Lipid A from various bacterial species.** Structural differences compared to the *E. coli* archetype arise from: the presence of phosphoryl substituents, degree of phosphorylation, and lipophilic chain lengths.

However, each Gram-negative bacterial species has unique structural features and composition for lipid A (Figure 5<sup>23</sup>).

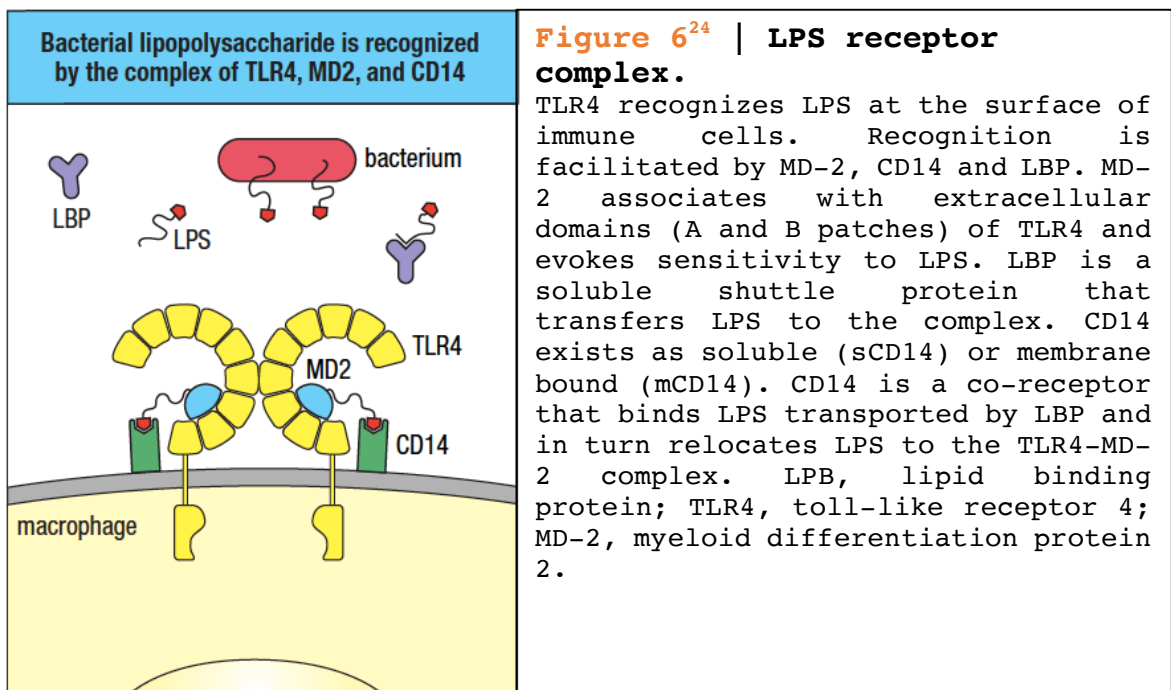
Fluctuations of the detailed structure emanate from: (1) the presence of phosphoryl substituents, such as a 4-amino-deoxy-L-arabinose and/or phosphoethanolamine linked axial at C-1 or C-4', (2) the degree of phosphorylation, (3) and importantly the highly variable nature of the lipids, with lipophilic chain lengths usually 6 to 18 carbon atoms in length. Also important are the type and position of the acyl groups. The acylation pattern of each hexosamine residue can have either a symmetric (3+3) or an asymmetric (4+2) distribution.<sup>22</sup>

Functionally, lipid A provides the anchor that binds LPS to the membrane with large numbers of saturated fatty acyl groups. This generates a gelatinous barrier of low fluidity and even impedes the infiltration of hydrophobic particles into the membrane. The two polysaccharide components interact with the extracellular environment and extend ~10 nm from the surface of the outer membrane. These heteropolysaccharide chains allow passage of small molecules for nutrient uptake, but are impermeable to larger molecules like proteins. This feature confines periplasmic proteins to prevent them from diffusing away. The barrier is additionally stabilized by LPS-associated cations that link adjacent molecules through salt bridges. Taken as a whole, the highly oriented and tightly cross-linked structure protects Gram-negative bacteria from a variety of host-defense molecules, thereby

permitting growth and survival within harsh environments or an infected host.

## B. The LPS Receptor Complex

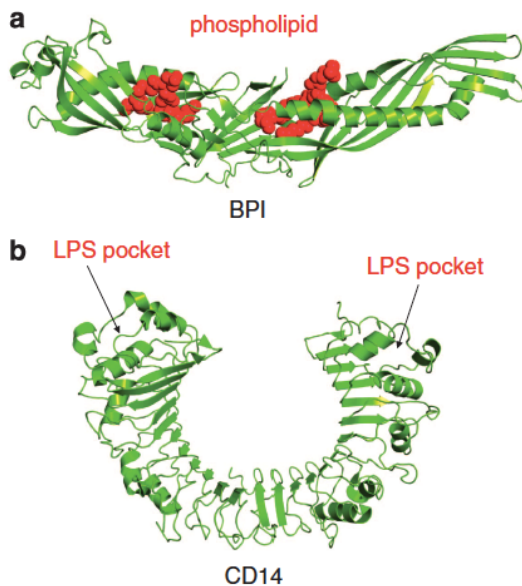
Accurate recognition of pathogen-associated molecular patterns (PAMPs) by pattern recognition receptors (PRRs) is the crux of the innate immune response.<sup>24</sup> An important receptor on the surface of immune cells such as monocytes/macrophages, neutrophils, B lymphocytes, myeloid dendritic and mast cells that recognizes LPS is toll-like receptor 4 (TLR4). As a homodimer, TLR4 requires the small myeloid differentiation protein-2 (MD-2) for recognition of LPS.<sup>24</sup> Other key proteins such as LPS binding protein (LBP) and CD14 facilitate the presentation of LPS to the TLR4-MD-2



complex (Figure 6<sup>24</sup>).<sup>24</sup> Once activated, TLR4 mobilizes adapter molecules within the cytoplasm of cells to propagate a signal.<sup>24</sup> In turn, the adapter molecules activate molecules within the cell to amplify the signal, which leads to the induction of genes that orchestrate the inflammatory response.

### 1. LBP & CD14

Above critical micellar concentrations, LPS forms large aggregates in aqueous environments due to its inherent amphipathic nature. LBP is a soluble shuttle protein that



avidly binds to LPS aggregates and facilitates the association between LPS and CD14.<sup>25</sup> As a complex, LBP-CD14 enhance the detection of LPS by extracting and monomerizing it prior to presentation at the TLR4-MD-2 complex.

LBP belongs to the lipid transfer family and to date its structure has not been reported. Bacterial and permeability-increasing protein (BPI),

**Figure 7<sup>26</sup> | BPI and CD14.**  
 (a) The crystal structure of BPI shares 48% sequence homology with LBP and has two phospholipid binding sites.  
 (b) Crystal structure of CD14 showing two LPS binding pockets.

another member of the lipid transfer family, shares 48% sequence homology with LBP and its structure has been elucidated (Figure 7<sup>26</sup>).<sup>27</sup> However, BPI does not transfer LPS to the TLR4-MD-2 complex, so functionally LBP has different capabilities than BPI.

Initially, CD14 was identified as a co-receptor that binds to LPS transported by LBP and in turn relocates bound LPS for presentation to the TLR4-MD-2 complex. Further investigations have demonstrated that CD14 also participates in activation by Gram-positive cell-wall components, such as peptidoglycan and lipoteichoic acid,<sup>28</sup> and mediates macrophage apoptosis.<sup>29</sup> Thus, CD14 functions as a PRR with broad ligand specificity by recognizing structural motifs of diverse microbial products.

CD14 exists in soluble (sCD14) or in anchored membrane (mCD14) form by a glycosylphosphatidylinositol tail.<sup>30</sup> Cells that do not express CD14, such as dendritic cells, are still able to respond to LPS by interacting with sCD14. During acute infection, serum levels of sCD14 and LBP rise<sup>31</sup> and anti-CD14 antibody protects primates from lethal LPS-induced septic shock.<sup>32</sup> Low concentrations of LBP intensify LPS response, whilst high concentrations inhibit LPS activity *in vitro* and *in vivo*.<sup>26</sup> Furthermore, sCD14 can also inhibit LPS response by facilitating LPS efflux from mCD14 and transporting it to

serum lipoproteins.<sup>33</sup> To sum, dual stimulatory and inhibitory mechanisms of LBP and sCD14 afford systemic anti-inflammatory effects, potentially hindering pathological systemic responses.<sup>34</sup> At the same time, LBP and sCD14 mechanisms can promote pro-inflammatory effects at local sites of infection, where they are needed.<sup>25</sup>

## **2. TLR4-MD-2 Complex**

The transmembrane TLRs were first discovered in *Drosophila*.<sup>35</sup> In humans, a family of 10 genes encodes TLR1-10, which are expressed by cells of the innate immune system. The 10 human TLR genes encode distinctive TLR polypeptides. Some TLRs are heterodimers of two polypeptides; others, such as TLR4, are homodimers (Table 2<sup>24</sup>). TLRs contain a variable extracellular domain for detection of PAMPs from an array of pathogens, including bacteria, viruses and fungi.<sup>36</sup> Toll Interleukin-1 Receptor (TIR) is the conserved cytoplasmic domain that conveys signal transduction intracellularly. TIR is critical for mediating protein-protein interactions between TLRs and five signal transduction adapter proteins, namely: myeloid differentiation primary response gene 88 (MyD88), TIR domain-containing adapter inducing IFN- $\beta$  (TRIF), TRIF-related adapter molecule (TRAM), TIR domain-containing adapter protein (TIRAP), and sterile  $\alpha$  and HEAT-Armadillo



Recognition of microbial products through Toll-like receptors						
	Receptor	Chromosome	Ligands	Microorganisms recognized	Cells carrying receptor	Cellular location of receptor
I	TLR1:TLR2 heterodimer	4	Lipopeptides	Bacteria	Monocytes, dendritic cells, eosinophils, basophils, mast cells	Plasma membrane
			Glycosylphosphatidylinositol	Parasites		
	TLR2:TLR6 heterodimer		Lipoteichoic acid	Gram-positive bacteria		
		Zymosan	Fungi			
	TLR10 homodimer and heterodimers with TLR1 and 2		Unknown		Plasmacytoid dendritic cells, basophils, eosinophils, B cells	Unknown
	TLR4 homodimer	9	Lipopolysaccharide	Gram-negative bacteria	Macrophages, dendritic cells, mast cells, eosinophils	Plasma membrane
II	TLR7 homodimer	X	Single-stranded viral RNAs	RNA viruses	Plasmacytoid dendritic cells, NK cells, eosinophils, B cells	Endosomes
	TLR8 homodimer		Single-stranded viral RNAs	RNA viruses	NK cells	Endosomes
	TLR9 homodimer	3	Unmethylated CpG-rich DNA	Bacteria DNA viruses	Plasmacytoid dendritic cells, B cells, eosinophils, basophils	Endosomes
III	TLR3 homodimer	4	Double-stranded viral RNA	RNA viruses	NK cells	Endosomes
IV	TLR5 homodimer	1	Flagellin, a protein	Bacteria	Intestinal epithelium	Plasma membrane

**Table 2<sup>24</sup> | Human TLRs recognize microbial ligands with pathogen associated molecular patterns (PAMPs).**

TLRs are encoded by 10 genes in humans from multiple chromosomes. TLRs acquired their nomenclature from the analogous receptor "Toll" found in the fruit fly *Drosophila melanogaster*. Differing PAMPs are found on distinct TLRs to confer variable ligand recognition. Some TLRs are heterodimers of two polypeptides and some exist solely as homodimers, such as TLR4.

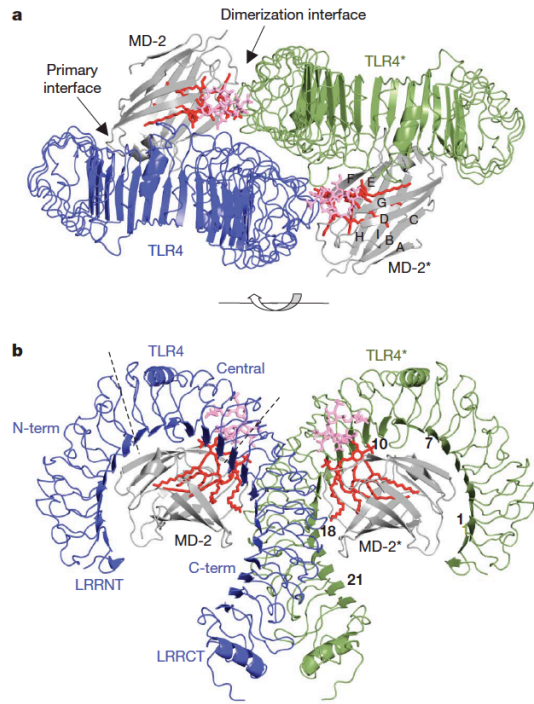
motif-containing protein (SARM).<sup>30</sup> Different combinations of adapter proteins are utilized by distinct TLRs, which in turn determines downstream signaling events. The signaling pathways of TLRs are well defined, however the precise mechanisms by which TLRs are activated upon ligand-binding are not entirely understood. Interestingly, TLR4 is the only recognized receptor that uses all five adapter proteins.<sup>30</sup>

The pathogen-recognition domains of TLRs consist of hydrophobic leucine-rich repeat (LRR) regions, which are

responsible for receptor dimerization and the characteristic horseshoe-like shape (Figure 8<sup>37</sup>). Variation in the composition and number of LRRs affords TLRs specificities for different microbial ligands.<sup>37</sup> LRR family proteins are classified into 7 subfamilies, which are characterized by conformations. Most LRR proteins contain uniform radii and  $\beta$ -sheet angles. However, the structure of some TLRs, including TLR4, substantially deviate from the consensus LRR conformations. They are divided by structural transitions into three subdomains: N-terminal, central, and C-terminal (Figure 8<sup>37</sup>).<sup>37</sup> Irregular LRR sequences in the central domain cause the structural deviations from other LRR family proteins. Furthermore, the subdomain boundaries of TLRs play

**Figure 8<sup>37</sup> | Crystal structure of TLR4-MD-2 bound to LPS.**

(a) Top view of LPS bound to TLR4-MD-2 complex. The primary interface is formed prior to LPS binding and the dimerization interface is created after LPS binding. (b) Side view of receptor complex. Lipid A is colored red and inner core region of LPS is colored pink. TLR4 is divided into N-terminal and C-terminal domains. LRRNT and LRRCT, leucine-rich repeat regions N- C-terminus respectively.



key roles in ligand binding, demonstrated by the primary contact interface of the TLR4-MD-2 complex.<sup>37</sup> The N-terminal and central domains of TLR4 provide charge complementary for binding MD-2, forming a stable 1:1 heterodimer via two distinct regions, the A and B patches respectively.<sup>37</sup> Notably, the TLR4-MD-2 complex is formed prior to binding LPS.

MD-2 is a soluble protein and can directly form a complex with LPS, yet LPS-MD-2 binding is enhanced with TLR4 association. Importantly, there is no evidence to suggest that TLR4 can independently bind LPS, emphasizing the significance of LPS recognition by MD-2. MD-2 has a  $\beta$ -cup fold structure formed by two anti-parallel  $\beta$ -sheets.<sup>37</sup> The  $\beta$ -sheets are separated from one another, which in turn exposes the hydrophobic interior for ligand binding. This generates a large internal pocket that is ideal for binding flat hydrophobic ligands, such as lipid A. In fact, the interaction between LPS and the TLR4-MD-2 complex occurs with high affinity, and the  $K_D$  is estimated to be 3-10 nM.<sup>38</sup>

### **3. Signal Transduction Pathway & Mediators**

As a homodimer, TLR4 binds MD-2 to form two 1:1 complexes. Then, sCD14 or mCD14 present LPS to the TLR4-MD-2 complex, which in turn propagates the signal by dimerization of the entire receptor complex. Such extracellular

recognition of LPS causes the cytoplasmic TIR domain of TLR4 to bind to a similar TIR domain of MyD88 (Figure 9<sup>24</sup>). Once TIR is bound to MyD88, a separate domain of MyD88 binds to the protein kinase IRAK4, whereupon it auto-phosphorylates itself and dissociates from the complex (Figure 9<sup>24</sup>). IRAK4 propagates the signal by phosphorylating the adapter protein

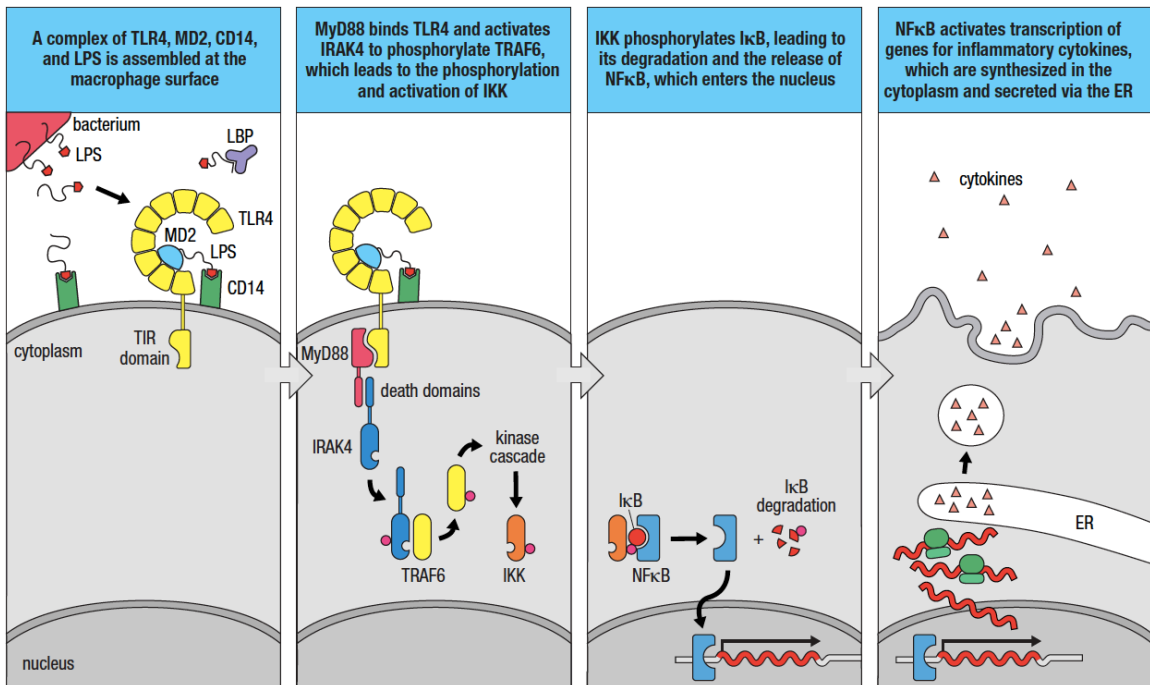


**Figure 9<sup>24</sup> | MyD88-dependent pathway induces NFκB to initiate transcription of cytokines upon LPS recognition by TLR4-MD-2 complex.**

Pathway from left to right: (1) LPS is detected by the TLR4-MD-2 complex. (2) Receptor complex dimerization causes cytoplasmic TIR domain to bind MyD88. (3) MyD88-associated IRAK4 auto-phosphorylates causing dissociation from MyD88. (4) Unbound IRAK4 phosphorylates TRAF6, which in turn induces a kinase cascade leading to activation of IKK. (5) Activated IKK phosphorylates IκB, leading to its degradation and subsequent release of transcription factor NFκB. (6) NFκB translocates into nucleus to initiate transcription of cytokine genes. (7) Cytokine mRNA is translated at ribosome and secreted extracellularly by the ER. **Abbreviations:** TIR, toll interleukin-1 receptor; IRAK4, interleukin-1 receptor-associated kinase 4; TRAF6, TNF receptor associated factor 6; IKK, inhibitor of κB kinase; IκB, inhibitor of κB; ER, endoplasmic reticulum.

TRAF6, which induces a cascade of events, eventually leading to activation of the kinase complex IKK (inhibitor of  $\kappa$ B Kinase). IKK performs the critical function of activating a transcription factor termed nuclear factor  $\kappa$ B (NF $\kappa$ B), which conducts significant operations to both innate and adaptive immune responses.<sup>39</sup> NF $\kappa$ B is held in an inactive state in a cytosolic complex with inhibitor of  $\kappa$ B (I $\kappa$ B). When IKK phosphorylates I $\kappa$ B, it releases NF $\kappa$ B from inhibition. Consequently, NF $\kappa$ B travels to the nucleus where it induces the transcription of genes for cytokines and numerous other proteins required to amplify the inflammatory response.<sup>39</sup>

#### **4. TRIF-dependent**

Alternatively, an MyD88-independent signaling pathway can be triggered by the recruitment of TRIF and TRAM.<sup>30</sup> These adapter molecules play a key role in activating interferon regulatory factor IRF3, which is essential for the expression of type I interferons, like IFN- $\beta$ .<sup>30</sup> Also, exuberant nitric oxide (NO) production results by activating the MyD88-independent (TRIF-dependent) pathway.<sup>40</sup> NO performs a major role in inflammatory pathogenesis as a signaling molecule and is thought to induce vasodilation.<sup>40</sup> To add, NF $\kappa$ B can be activated by the TRIF-dependent pathway, but in a later-phase. It is speculated that subcellular localization of TLR4

distinguishes the activation of the two signaling pathways. For instance, recognition of LPS at the plasma membrane activates the MyD88-dependent pathway, but in contrast, recognition of LPS at the endosome initiates the TRIF-dependent pathway. Nonetheless, induction of either IRF3 or NFκB activates the transcription of genes, which for the anti-viral response are type I IFNs and in the pro-inflammatory response, TNFα.

## **5. TNFα**

NFκB induces the transcription of TNFα and other pro-inflammatory cytokines including: IL-1β, IL-6, IL-8, IL-12 and IL-23.<sup>41</sup> Of these, TNFα is one of the most important soluble mediators of inflammation. It is responsible for an array of signaling events and is mostly generated from activated macrophages/monocytes.<sup>42</sup> TNFα is produced rapidly and can be detected within 15 minutes of LPS exposure in cell culture and *in vivo* peaks at 1.5 hours.<sup>43</sup> TNFα causes contrasting effects to endothelial cells of blood vessels in the infected tissues.<sup>44</sup> In a systemic infection, macrophages in the liver and spleen secrete TNFα into the bloodstream for systemic circulation. The result is decreased blood flow from vasodilation and diffuse leakage of plasma. TNFα released into the bloodstream also causes the liver to secrete acute-

phase proteins, which include Mannan-binding lectin and C-reactive protein. Both are critical to complement pathways and exacerbate the inflammatory response.

## **6. The Coagulation Cascade**

In localized infections, TNF $\alpha$  secretion causes blood flow to increase and endothelia to produce platelet-activating factor, which clots blood and blocks nearby vessels.<sup>45</sup> This induction of the coagulation cascade obstructs pathogens from entering the bloodstream, thereby preventing their spread. However, this process can impede delivery of oxygen to the tissues and can induce further inflammatory injury indirectly through the response to hypoxemia. Usually, induction of the coagulation pathway induces anticoagulant mechanisms to limit its progression. However, when the infection is diffuse, as in sepsis, an imbalance of the procoagulant and anticoagulant systems develop, generating a sustained hypercoagulable state.<sup>46</sup> Systemic widespread clotting depletes coagulation proteins and platelets from the blood. This process can lead to a bleeding complication syndrome called DIC. Clinically, DIC is increasingly common as a patient progresses from severe sepsis to septic shock.<sup>46</sup> Simultaneously, microvascular thrombosis develops contributing to end-organ damage.<sup>46</sup>

Without intervention, lack of blood flow to the organs causes multiple organ failure, which ultimately determines the septic patients prognosis.

Overall, multiple and diverse pathways lead to a hyper-activated immunological response that manifests end-organ damage in sepsis. LPS itself is nontoxic but its adverse effects emanate through systemic activation of host-derived inflammatory mediators. Attempting to block a single cytokine, like TNF $\alpha$ , would be inadequate due to the large quantity and diversity of cytokines produced by activated cells. Consequently, the path towards generating enhanced therapeutics for the septicemic patient does not lie with interrupting downstream incidents, but by blocking the initial signaling events of the cascading inflammatory response.

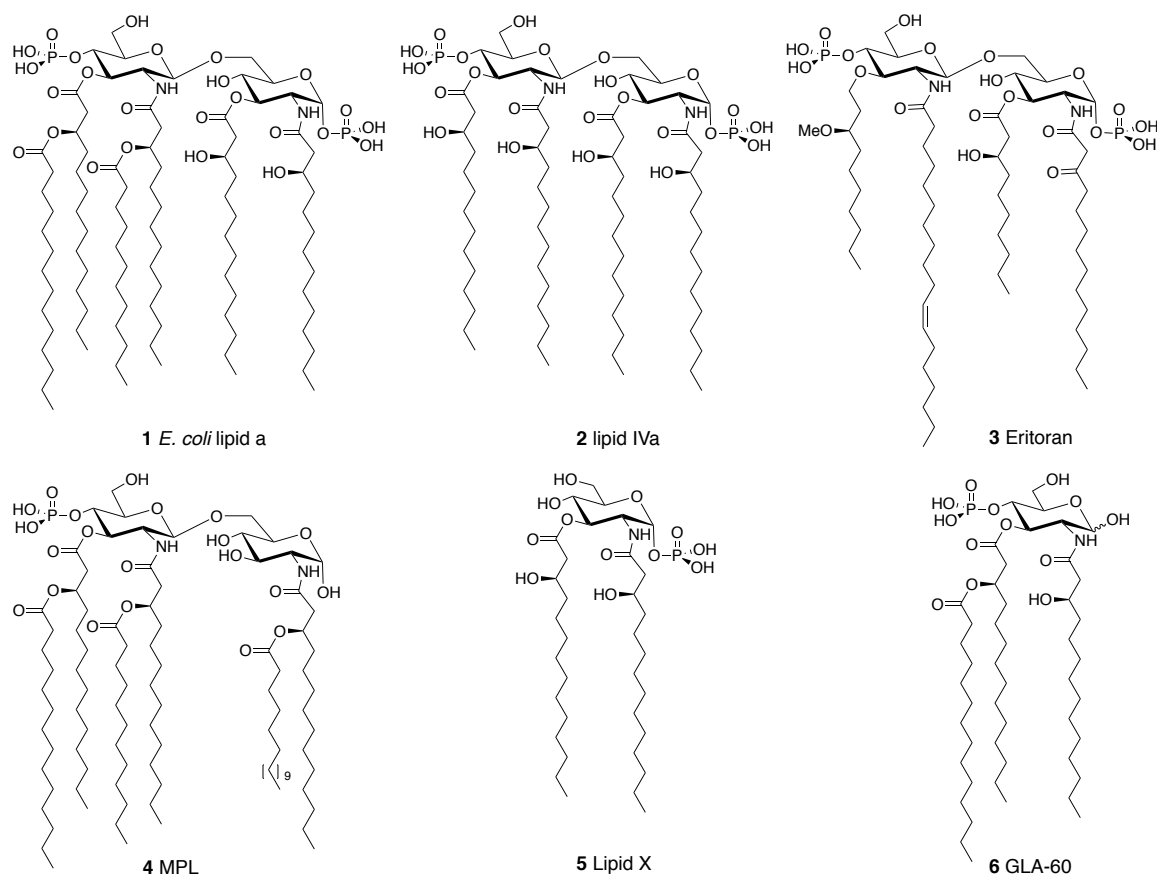
### ***C. Lipid A Analogues***

Synthesis of lipid A analogues first emerged with the ambition to understand the chemical structures that were principally responsible for endotoxic activity in sepsis.<sup>47</sup> Some of the most informative studies of structure-activity relationships of lipid A have utilized synthetic and natural antagonist.<sup>48</sup> In particular, the use of a naturally occurring precursor from the constitutive biosynthesis pathway in *E.*



*coli* called lipid IV<sub>a</sub> (**2**) and a nonpathogenic lipid A molecule from *Rhodopseudomonas sphaeroides*. The latter of which served as the structural basis for the drug candidate Eritoran (**3**). In phase III clinical trials, Eritoran (**3**) did not perform better than existing treatments for sepsis.<sup>49</sup> However, it did demonstrate efficacy in combating cytokine storm induced from strains of influenza in animal models.<sup>50</sup> Another key contributor to our continued understanding was isolation and characterization of 3-O-desacyl-4'-monophosphoryl lipid A (MPL) (**4**).<sup>51</sup> Comparison of MPL derivatives provides clues for

**Figure 10 | Structure of *E. coli* lipid A and derivatives.**  
**(1)** Structure of agonistic *E. coli* lipid A. **(2-5)** Antagonist to LPS signaling at TLR4-MD-2 complex.



chemical alterations that direct endotoxicity and adjuvanticity. Development of the less endotoxic MPL has led to its widespread use as a component of numerous licensed vaccines, including HBV and papilloma, and has been proven both safe and effective.<sup>51</sup> Detoxification was achieved by acid hydrolysis of the 1-O-phosphono group followed by base hydrolysis of the 3-hydroxytetradecanoly group to yield MPL (**4**). In addition, studies revealed that lipid IV<sub>a</sub> (**2**) has conflicting properties between human and murine cells.<sup>51</sup> It was shown to inhibit the induction of inflammatory cytokines in human cells co-treated with LPS or lipid A. However, in murine cell lines lipid IV<sub>a</sub> (**2**) was shown to be a potent inducer of inflammatory cytokines. These species-specific results were later explained by structural differences between human and murine TLR4-MD-2 complexes. Specifically, lipid IV<sub>a</sub> (**2**) caused contrasting effects on dimerization of the TLR4-MD-2 receptor complex, which is required for activation of downstream signaling. Expectedly, lipid IV<sub>a</sub> (**2**) was shown to promote receptor dimerization in murine, but not human TLR4-MD-2 complexes.

Activation of the TLR4-MD-2 complex can lead to distinct signaling pathways namely; the MyD88-dependent or the TRIF-dependent pathways. Induction of the MyD88-dependent pathway causes production of proinflammatory cytokines such as TNF $\alpha$ ,

whilst TRIF-dependent pathway activation leads to NO and IFN- $\beta$  production. Teasing apart the structural determinants of lipid A that induces the former or the latter has implications in determining subsequent endotoxicity or adjuvanticity.<sup>51</sup> Previously stated, CD14 is a PRR that directly binds to LPS and chaperones the formation of the dimerized TLR4-MD-2 complex. At low concentrations of LPS, CD14 plays an increased role in formation and subsequent receptor dimerization leading to induction of the MyD88-dependent pathway. Albeit, CD14 is not essential for this induction when LPS is in higher concentrations. CD14 is also required for TLR4 endocytosis and internalization of the entire receptor complex into the endosome, thereby inducing the TRIF-dependent pathway.<sup>51</sup> It has been demonstrated that TLR4 antagonist, such as lipid IV<sub>a</sub> (2) and Eritoran (3), strongly interact with CD14, thereby inhibiting re-localization of the receptor complex.<sup>52</sup>

### **1. Monosaccharide Mimetics**

Researchers have attempted to separate beneficial immunopharmacological attributes from adverse pathophysiological endotoxic properties of lipid A by performing structure-activity analyses of simplified structures. Lipid A has a basic endotoxic structure of an amphipathic molecule, with distinct hydrophilic and

hydrophobic domains. The association of a polar backbone supporting an apolar region is vital for its antagonistic or agonistic properties. However, the specific structure of the glucosamine disaccharide backbone is seemingly not stringent in directing which biological activity will result. Synthetic lipid A derivatives with one of the glucosamine disaccharide residues replaced with acyclic or pseudo-peptides have contained similar activities of *E. coli* lipid A, whilst others have demonstrated antagonistic properties.<sup>53</sup> Interestingly, both or at least one phosphate, or bioisotere of, substituents at the anomeric or 4'-carbons seem to be a prerequisite for substantial biological activity.

The approach of dividing lipid A into reducing and non-reducing halves has been utilized to develop therapeutics. Lipid X (**5**) is a biosynthetic precursor of lipid A with a structure that corresponds to the reducing monosaccharide half, which consist of 1-phosphoryl, diacyl 2-N-, 3-O-, hydroxytetradecanoyl-D-glucosamine.<sup>52</sup> Synthesized structures that emulate Lipid X (**5**) have shown to lack both endotoxic and immunostimulatory properties. To add, Lipid X (**5**) derivatives were often antagonist of lipid A or LPS.<sup>52</sup> In comparison, divided lipid A analogues of the non-reducing half also produce attenuated endotoxic activities. For example, GLA-60 (**6**) is a lipid A analogue of the non-reducing

section and displays a 4-phosphoryl D-glucosamine monosaccharide moiety with three acyl chains of 12-14 carbons in length. Interestingly, GLA-60 (**6**) based compounds are relatively potent adjuvants, provide non-specific protection from bacterial and viral infections and are tumor regressive.<sup>54</sup> Furthermore, current studies have revealed monosaccharide lipid A analogues as potential adjuvants for cancer treatments with multiple phase 1 trials underway.<sup>55-65</sup>

## **2. Antagonizing LPS-Induced Dimerization**

Despite substantial data on the activity of both isolated and synthetic lipid A derivatives, there unfortunately is no universal correlation between the chemical structure of lipid A and its activity in the TLR4-MD-2 complex. However, elucidation of the crystal structure of the TLR4-MD-2 complex bound to antagonistic lipid IV<sub>a</sub> (**2**) or Eritoran (**3**) and agonistic *E. coli* lipid A (**1**) has contributed a better understanding of structural requirements for the receptor complex (Figure 11<sup>37</sup>).<sup>37</sup>

Previously stated, TLR4 as a homodimer binds MD-2 to form two 1:1 complexes that then dimerize upon ligand binding. LPS binding induces dimerization by creating an additional binding interface between TLR4 and MD-2. To distinguish the secondary dimerized heterotetrameric TLR4-MD-2\* complex from

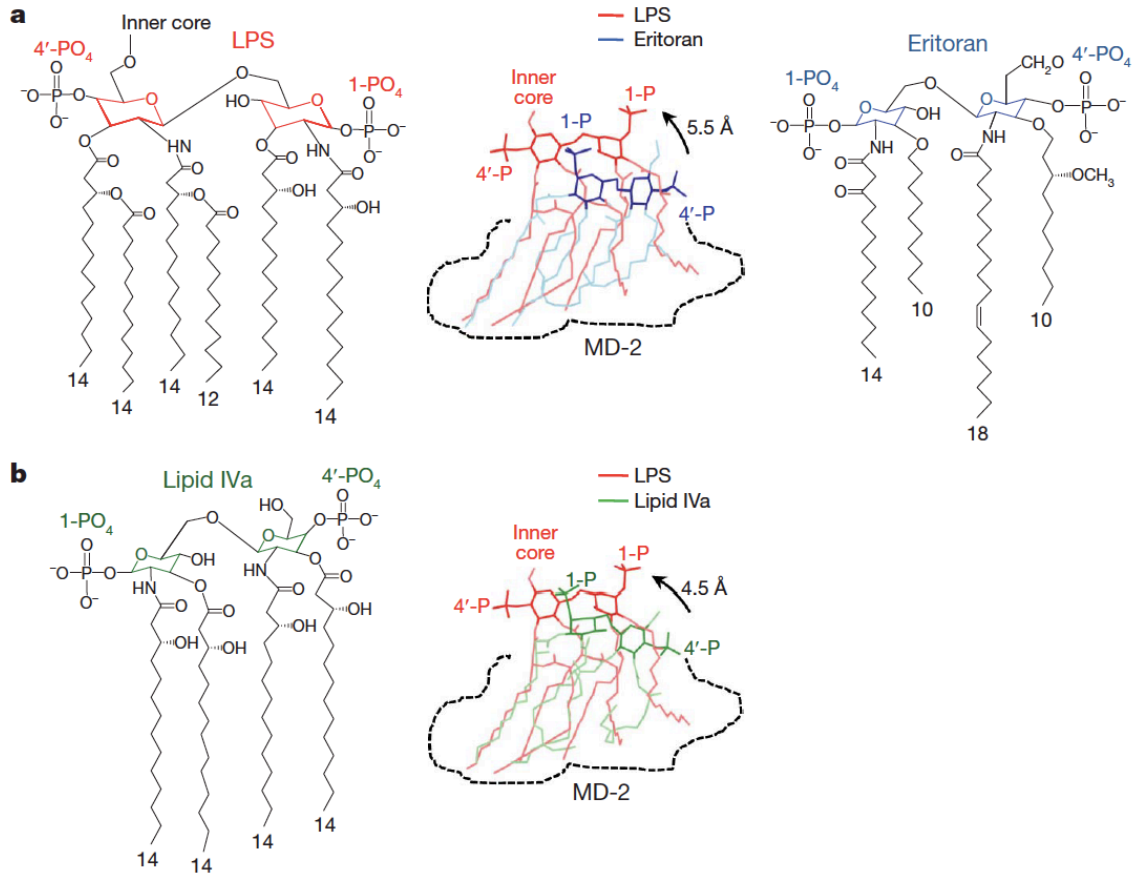


**Figure 11<sup>37</sup> | LPS antagonist shift the anomeric phosphate.** The size of the MD-2 pocket is unchanged after binding agonistic or antagonistic lipid A. Added space for lipid binding displaces the anomeric phosphate upwards ~5Å, allowing interaction with nearby positive charges on TLR4 and TLR4\*. (a) Comparison of LPS and Eritoran binding. (b) Comparison of LPS and lipid IVa binding.

primary TLR4-MD-2, an asterisk is utilized. Accordingly, the carbon chains of lipid A interact with the hydrophobic pocket of MD-2. Five of the six lipid chains of agonistic LPS are enclosed by the hydrophobic pocket and the sixth is uncovered to the surface of MD-2 (Figure 12<sup>37</sup>), whilst all four lipid chains of lipid IV<sub>a</sub> (2) are buried (Figure 11<sup>37</sup>).<sup>37</sup> The sixth lipid chain of LPS forms a hydrophobic interaction with

phenylalanine residues of TLR4\*. This provides an explanation why previous studies have shown that six lipid chains are optimal for activation of TLR4 signal transduction when compared to derivatives with fewer lipid chains.<sup>21</sup> The ester and amide groups that connect the lipophilic chains to the polar head group of lipid A are also exposed to MD-2 in binding agonist *E. coli* lipid A (**1**). However, these interactions generate a minimal number of weak bonds with TLR4\* and TLR4.<sup>37</sup> This is supported by biological activity of lipid A analogues, whereupon more robust ethers have been

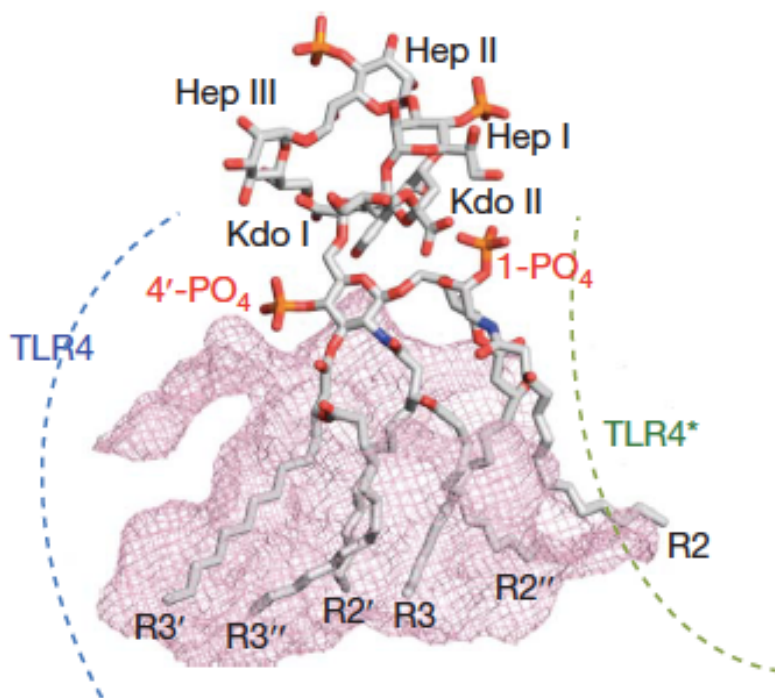


**Figure 12<sup>37</sup> | Dimerization of receptor complex with LPS.** Lipophilic chains interact with the hydrophobic pocket of MD-2. The exposed R2 chain interacts with TLR4\* at dimerized interface. The MD-2 pocket is depicted with the mesh. Primary and secondary dimerized interface are depicted TLR4 and TLR4 and TLR4\*, respectively.

substituted.<sup>21</sup> The two phosphate groups bind to residues of TLR4-MD-2 and at the dimerization interface of TLR4\*, thus supporting the formation of a stable (TLR4-MD-2)<sub>2</sub> dimerized complex. Both the 1-phosphate and 4'-phosphate of lipid A bind to positive patches on TLR4 and TLR4\* (Figure 13<sup>37</sup>). The

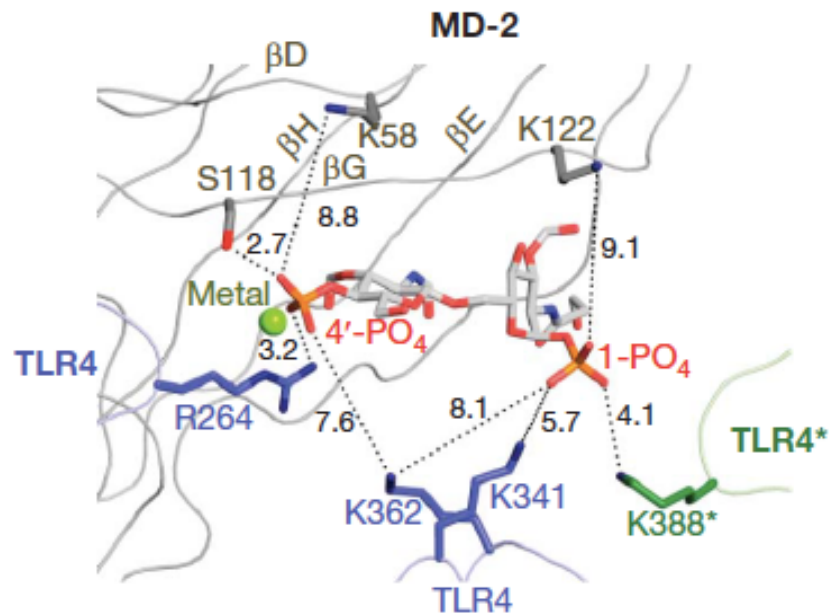


**Figure 13<sup>37</sup> | Both phosphates of LPS lipid A interact at dimerized receptor complex.**

The 1-phosphate and 4'-phosphate conduct dimerization by binding positively charged arginine and lysine residues of TLR4 and TLR4\*. These two ionic interactions are critical elements for activation of TLR4-MD-2 complex. Removal of one phosphate group greatly reduces endotoxicity.

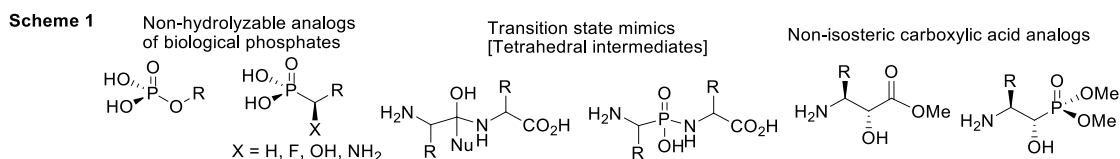
significance of these two interactions has been established. As demonstrated with MPL (4), removal of one phosphate group greatly reduces the endotoxicity of LPS. Secondly, when the positively charged patch of TLR4\* was mutated to an alanine residue, NFκB and IFN-β activity was abolished.<sup>66</sup> This finding



suggest that the 1-phosphate of lipid A is essential for activation of both MyD88-dependent and TRIF-dependent pathways. Thus, subtle structural changes at the anomeric phosphate of lipid A could illuminate the path towards guided activation between endotoxicity and adjuvanticity.

## D. Phosphonates

The phosphate group  $[(HO)_2P(=O)OR]$  is a fundamental component of all living systems. It is essential for molecular replication, cell biochemistry, signaling pathways, and regulation of metabolic processes.<sup>67</sup> Phosphonate analogs of phosphates, wherein the phosphate ester bond has been replaced with the hydrolytically stable phosphonate  $[(HO)_2P(O)R]$  (R=carbon residue), often contain enticing physiological properties (**Scheme 1**).<sup>68-72</sup> An alpha substituent (X) can be used to return the pKa of the phosphonic acid to



the values typical of the corresponding phosphate ester. In addition, the tetracoordinate phosphoryl group is well recognized as an excellent mimic for the tetrahedral transition state of ester and amide hydrolysis.<sup>73</sup> More

surprisingly, phosphonic acids can successfully act as non-isosteric replacements for carboxylic acids.<sup>74</sup>

### **1. Phosphono-sugar Analogues**

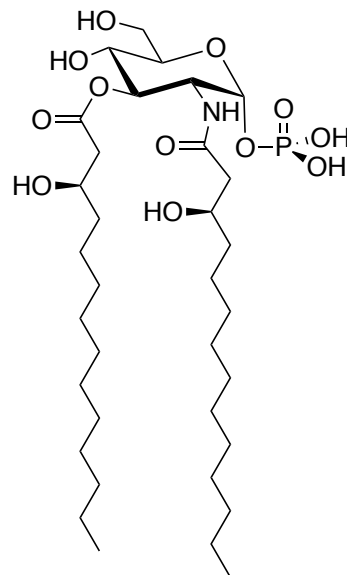
Phosphonates have become increasingly useful in the development of tools for biological investigation and the formulation of novel compounds for medicinal chemistry. For instance, phosphonate derivatives that contain additional functionality in the carbon chain are extremely versatile by exhibiting activities as receptor agonists-antagonists<sup>75</sup> and herbicidal, antibacterial, and antiviral agents<sup>76-80</sup>, usually through the inhibition of specific enzymes.<sup>81,82</sup>

There are many examples of phosphono-sugars where the phosphonate is located on a ring substituent. Such compounds are important in the development of non-hydrolysable phosphonate mimics of bioactive carbohydrate phosphates, such as nucleotides.<sup>83-85</sup> Research in this area has resulted in several examples of biologically relevant molecules.

### III. Results & Discussion

#### 1. Development of Lipid X Mimetics

Structural properties of the TLR4 receptor complex provide insight into LPS binding and subsequent dimerization for potentiating biological responses. Numerous lipid A variants have been synthesized to date and demonstrate that subtle changes in the length of the lipophilic chains, degree of phosphorylation of the polar backbone and modification of the disaccharide moiety

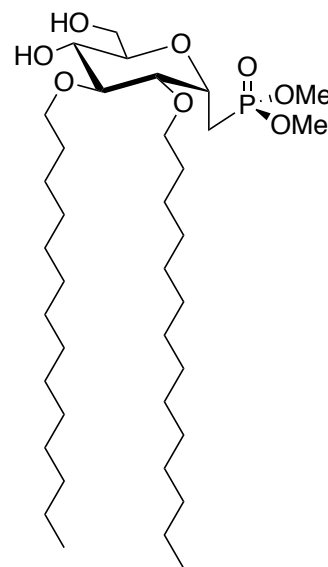


**5 Lipid X**

can profoundly alter biological activity.<sup>48</sup> The monosaccharide Lipid X (**5**) has been shown to block priming of TLR4-dependent neutrophils and antagonizes LPS signaling.<sup>52</sup> Furthermore, previous studies suggest that dual targeting of MD-2 and CD14 is accomplished with Lipid X (**5**) based analogues.<sup>52</sup> A successful approach to downregulating LPS signaling would involve compounds that compete with LPS binding to MD-2 and CD14, consequently inhibiting inflammatory signal transduction pathways by impairing LPS-initiated receptor dimerization and internalization. Due to its anti-endotoxic

activity, coupled with a simplified monosaccharide moiety that would prove more cost effective and more readily scalable, we selected Lipid X (**5**) based derivatives to synthesize.

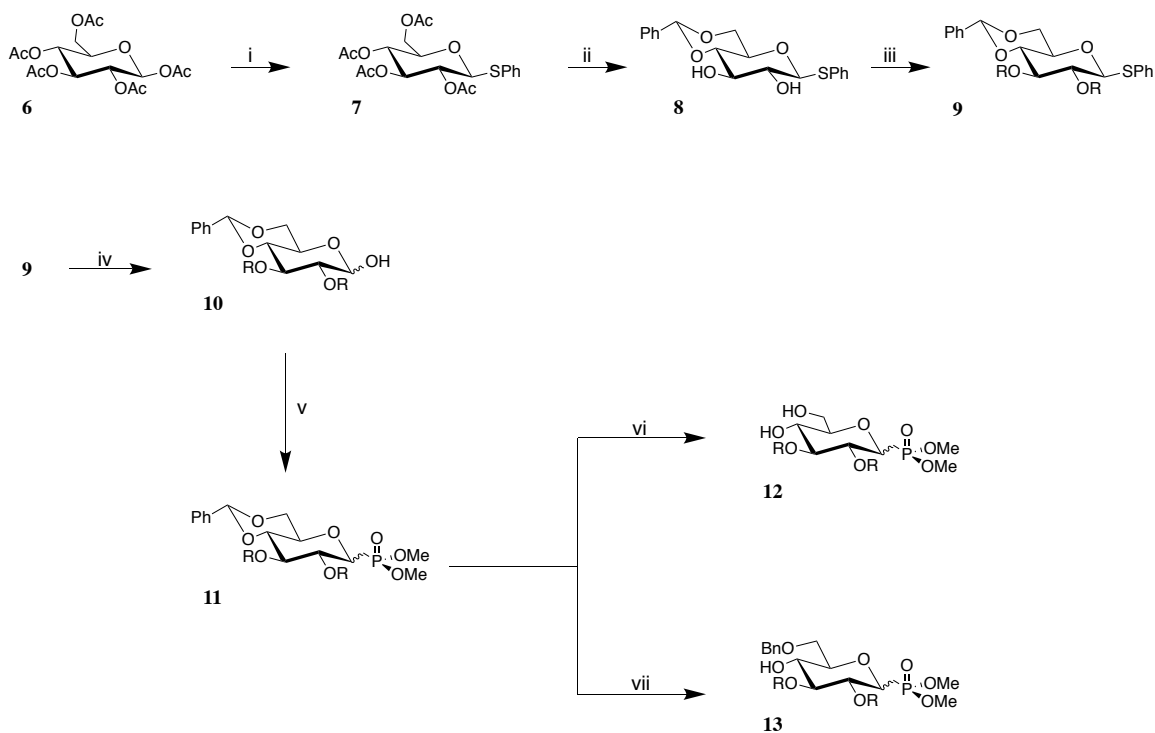
Monosaccharide based TLR4 receptor targeting could also afford compounds with enhanced water solubility. Previously synthesized lipid A mimetics suffer from poor solubility in aqueous media<sup>86</sup>, which is essential for improved bioavailability and a more favorable pharmacokinetic profile. Significantly, gaining structural insight to guide future explorations in distinguishing endotoxicity and adjuvanticity are paramount to progress lipid A analogues. To date, C-glycosylated phosphono-glucoside mimetics of Lipid X have not been explored. Thus, we employed traditional carbohydrate chemistry techniques to develop a non-hydrolysable phosphonate mimic of Lipid X (**12 $\alpha$** ) and assessed its biological activity for antagonizing LPS *in vitro*.



**12- $\alpha$**

## 2. Overall Synthesis

Synthesizing TLR4-MD-2 receptor antagonists by incorporating a phosphonate onto a ring substituent will generate the non-hydrolysable Lipid X mimetic (**Scheme 2**). The proposed synthesis begins with the formation of peracetylated-thio- $\beta$ -D glucoside (**7**) from penta-acetylated



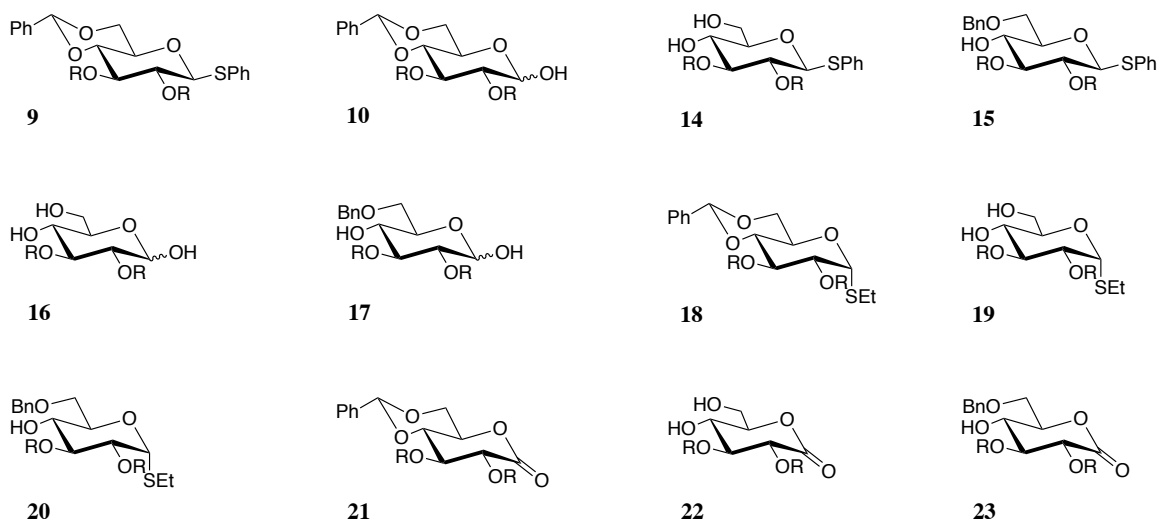
### Scheme 2 | Reagents and Conditions (R = C<sub>14</sub>H<sub>29</sub>)

(i) PhSh, BF<sub>3</sub>·Et<sub>2</sub>O, DCM, rt, 4h, (78%); (ii) 1. NaOMe, MeOH/DCM 1:10, 0 °C, 1h, (99%); 2. PhCH(OMe), pTsoH, DMF, 60 °C, 4h, (80%); (iii) NaH, tetra-*N*-butylammonium iodide, Bromo-tetradecane, DMF/THF 2:3, 40°C, 24h, (78%); (iv) 1. *N*-IS, 1.1 eq. TFA, DCM, rt, 1h; 2. Piperidene, rt, (84–94%); (v) THF, NaH, ((MeO)<sub>2</sub>(O)P)<sub>2</sub>CH<sub>2</sub>, rt, 2–24h, (48–54%); (vi) 15% TFA in wet DCM, rt, 1h, (77%); (vii) THF, NaCNBH<sub>3</sub>, 2 N HCl/Et<sub>2</sub>O, rt, 30 min., (84%).

glucose (**6**) as depicted,<sup>87</sup> deacetylation of the peracetylated-thio- $\beta$ -D-glucoside (**7**) will generate the tetrol, which will then be protected as a benzylidene. The resulting diol (**8**) is alkylated creating both lipophilic chains (**9**). Hydrolysis of the thiophenol forms the anomeric hydroxy (**10**) that is subjected to Horner-Wadsworth-Emmons reaction conditions to introduce the phosphonate moiety (**11**). Hydrogenolysis or selective C-4 ring cleavage of the benzylidene protecting group will afford novel phosphono-sugar (**12**) and (**13**) analogues of lipid X. The proposed route also allows for divergent chemistry to produce a library of compounds (**Scheme 3**) to more fully explore structure activity relationships of Lipid X.

**Scheme 3 | Our library of monosaccharide mimetic compounds synthesized.**

R = C<sub>14</sub>



### 3. Protecting Group Strategy

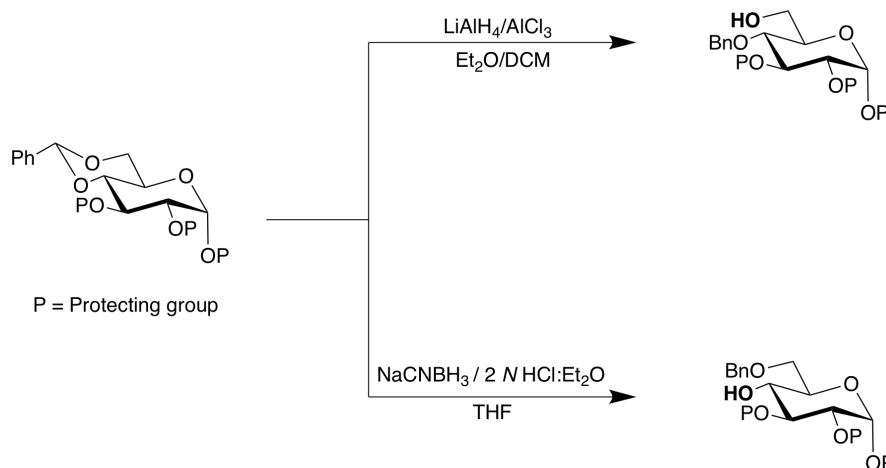
Strategical implementation of protecting groups is an important component for any total synthesis of organic molecules, but this is especially true in carbohydrate chemistry. Carbohydrates present a large number of poly-functionalized groups. Most of them are of the same sort, that is in the form of free hydroxyls. Success depends upon differentiating the relative reactivity of the hydroxyls, which are reflected by electronic and conformational factors. The different reactivity of the hydroxyls manifest from namely: one primary (C-6), several secondary (C-2, -3, & -4), and an acetalic group at the anomeric center. The most reactive is the hydroxyl at the anomeric carbon followed by the primary alcohol at C-6. The secondary hydroxyls contain varying reactivity due to their equatorial or axial orientations. This feature of carbohydrates necessitates regioselective strategies, which can be arduous at times.

Protecting groups also impart other effects of the compound. They can alter the reactivity of a molecule and can also participate in the reaction itself, therefore affecting the stereochemical outcomes. Ideally, it should be possible to introduce and remove more permanent protecting groups with regiocontrol and high efficiency. They should be stable under

conditions used for the addition and removal of temporary protecting groups. Acetals confer this stability and in addition contain efficient introduction and deprotection properties, for instance simultaneous protection of C-4 and C-6 hydroxyls. Of the acetals, we employed benzaldehyde dimethyl acetal  $\text{PhCH}(\text{OMe})_2$  under standard acetalization conditions with  $\text{pTsOH}$  as the acid catalyst to produce compounds **(9)** and **(18)** in good yields.

An added advantage of the benzylidene acetal as a protecting group is the number of subsequent modifications that can yield various protecting group patterns (**Scheme 4**).

**Scheme 4 | Examples of reductive cleavage of benzylidene acetals.**



Selective reduction to yield benzyl ethers and free hydroxyl groups are readily utilized with a hydride reagent in combination with a Lewis acid. Combination of  $\text{LiAlH}_4/\text{AlCl}_3$  would afford 4-O-benzyl derivatives unveiling the primary

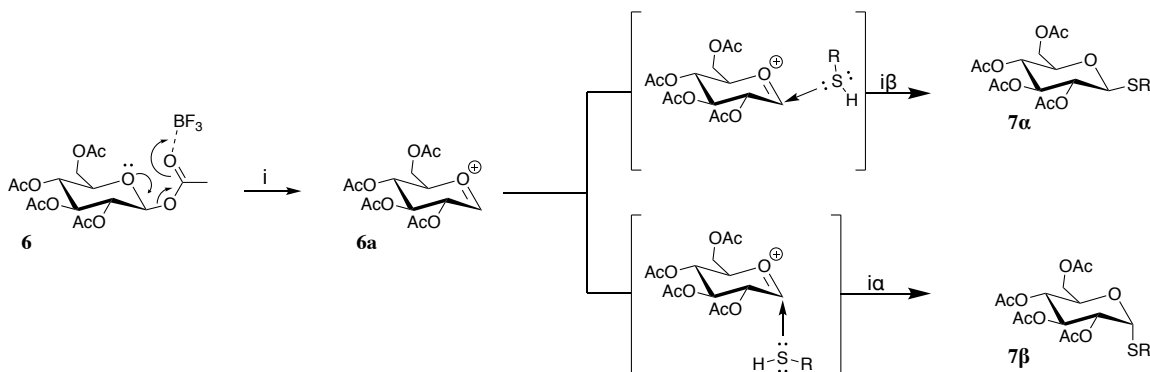


alcohol at C-6, whilst NaCNBH<sub>3</sub>/HCl will give the opposite 6-O-benzyl ether, as we demonstrated in formulating compounds **13 $\alpha$** , **13 $\beta$** , **15**, **20** and **23**.

Also, complete cleavage of benzylidene acetals can be achieved under mild conditions with 15% TFA in wet DCM or with Pd catalyzed H<sub>2</sub> reduction. For ease of use, we utilized 15% TFA in DCM for complete benzylidene cleavage to produce 4,6-diol compounds **12 $\alpha$** , **12 $\beta$** , **14** and **22** in good yields. Not presented in this embodiment of work, but a useful synthetic tool is employing benzylidene acetals under oxidative conditions, usually NBS in CCl<sub>4</sub>, to yield benzoyl ester protected halogen derivatives.

#### **4. Anomeric hemiacetal protection**

Thioglycosides are readily prepared by nucleophilic substitution at the anomeric center, commonly from anomeric acetates by reaction with thiols in the presence of a Lewis acid, such as BF<sub>3</sub>·Et<sub>2</sub>O (**Scheme 5**). Thioglycosides exhibit remarkable stability and withstand diverse chemical modifications, leaving the thioglycoside functionality intact. Most carbohydrate protecting group manipulations, including benzylidene introduction and selective cleavage,



**Scheme 5 | Thioglycoside Anomeric Protection.**

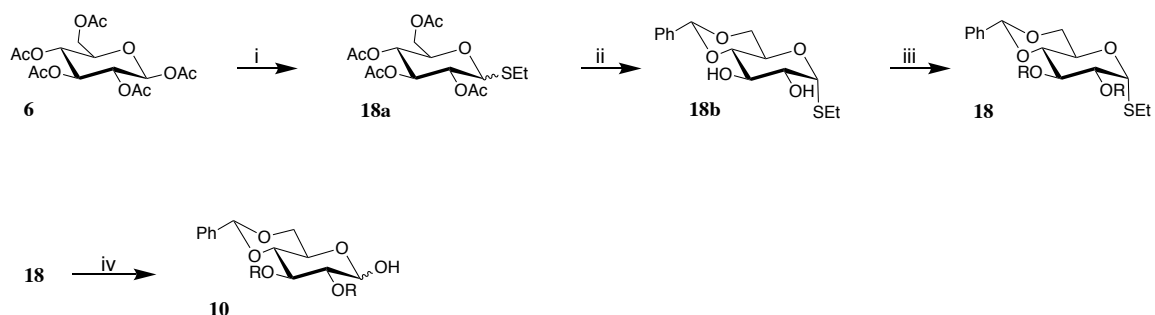
**R = Ph or Et**

(i) Mechanism of to generate thioglycosides from penta-acetylated-β-D-glucose, depicting the formation of the α or β anomers. We utilized BF<sub>3</sub>·Et<sub>2</sub>O in the presence of ethanethiol and thiophenol. Thiophenol was found to be β-selective, whilst ethanethiol generated a mixture of anomers.

can be performed. In addition, thioglycosides can serve as glycosyl acceptors to construct oligosaccharides.

Thus, we protected the anomeric carbon of (6) with thiophenol to produce (7) prior to 4,6-*O*-benzylidene (8) formation. However, in a subsequent step for our synthesis, thiophenol proved its stability. To generate the phosphono-sugar, the anomeric thio-protecting group needs to first be hydrolyzed. We found this step to be difficult using commonly applied methods. We observed the conventional strategies using *N*-bromo- and *N*-iodo-succinimide, and *N*-iodosaccharin in the presence of minute amounts of H<sub>2</sub>O to be unsuccessful. We also tried catalytic auric chloride as a strategy to activate thioglycoside donors, which had recently been reported.

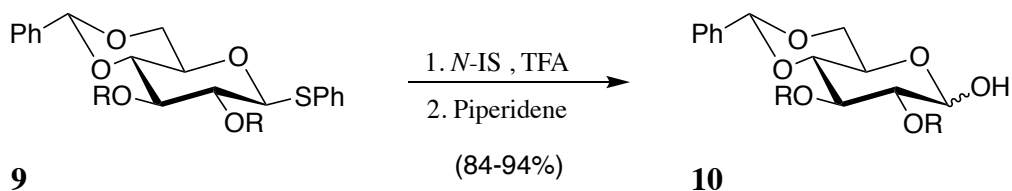
Unfortunately, this method also proved unsuccessful. The over-arching problem observed in these reactions were with solubility. Addition of tiny amounts of H<sub>2</sub>O, required for hydrolysis in these reaction methods, resulted in the starting thioglucoside (**9**) to rapidly precipitate from solution in a variety of solvents (DCM, Et<sub>2</sub>O, THF, dioxane, acetone and others). This issue lead us to generate the more polar anomeric protection of ethanethiol (**18**). In comparison, ethanethiol derivatives produced higher yields in each reaction step previous to anomeric hydrolysis (**Scheme 6**). Ethanethiol derivatives were found to be more soluble compared to thiophenol compounds at the anomeric hydrolysis step. However, yields were low using NBS and 2,6-lutidine in dioxane and the starting material (**18**) still demonstrated some solubility issues.



**Scheme 6 | Reagents and Conditions (R = C<sub>14</sub>H<sub>29</sub>)**

(i) EtSh, BF<sub>3</sub>·Et<sub>2</sub>O, DCM, rt, 6h, (83% as α/β mixture); (ii) 1. NaOMe, MeOH/DCM 1:10, 0 °C, 1h, (99%); 2. PhCH(OMe), pTsoH, DMF, 60 °C, 4h, (88%); (iii) NaH, tetra-*N*-butylammonium iodide, Bromotetradecane, DMF/THF 2:3, 40°C, 24h, (83%); (iv) 1. *N*-IS, 15% TFA in DCM, rt, 1h; 2. Piperidine, rt, (84-94%); (v) THF, NaH, ((MeO)<sub>2</sub>(O)P)<sub>2</sub>CH<sub>2</sub>, rt, 2-24h, (48-54%); (vi) NBS, 2,6-lutidine, dioxane, rt, 6h, (53%). **Note:** α-anomer was separated and utilized for (ii).

Eventually, we did develop a method to alleviate the solubility issues encountered by the particularly hydrophobic compounds **(9)** and **(18)**. To complete this step in the synthesis, the thioacetal **(9)** was hydrolyzed by treatment with NIS and dry TFA in DCM, followed by addition of piperidine to cleave the intermediate trifluoroacetate and afford the hemiacetal **(10)** as a 1:1 anomeric mixture in high yield (~90%). This step permitted hydrolysis without the use of H<sub>2</sub>O, which evoked our problems with solubility.



**Scheme 7 | Deprotection of Thioglycoside.**

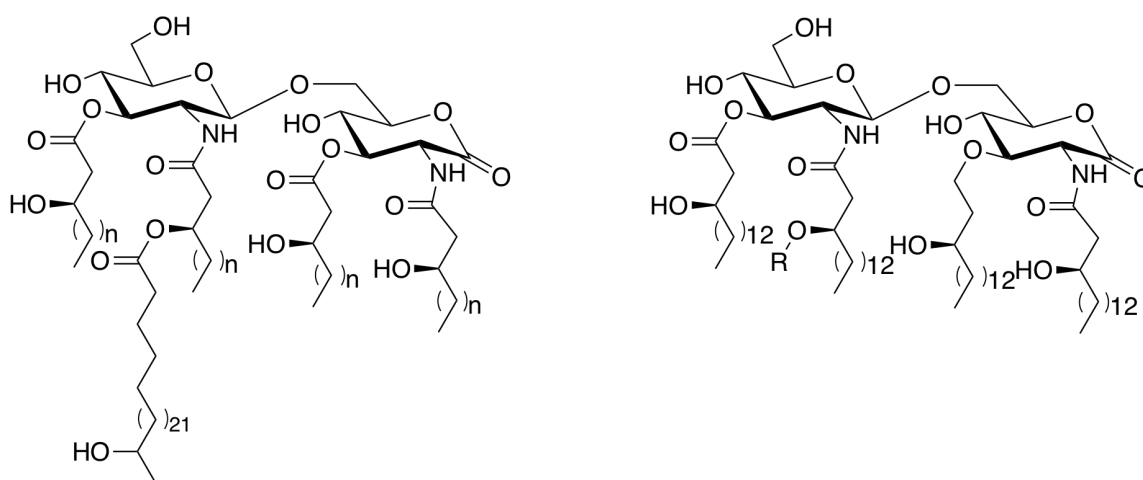
*Reagents and Conditions:* 1. N-IS, 1.1 eq. TFA, DCM, rt, 1h; 2. Piperidine, rt, (84-94%)

## 5. Synthesis of lactone derivatives

Lipid A from the LPS of the nitrogen fixing bacterial species *Rhizobium sin-1* (**(24)**) is structurally distinct, in comparison to endotoxic *E. coli* lipid A. It is completely devoid of phosphates, has a very long chain fatty acid (27-hydroxyoctacosonic acid), and contains a D-gluconolactone moiety at the reducing end (**Scheme 8**). Interestingly, compound **(24)** and a synthetic disaccharide derivative **(25)**

have shown to be potent in antagonizing LPS-induced cytokine production in human macrophage cells by inhibiting both TRIF- and MyD88-dependent pathways.<sup>21</sup> Intriguingly, monosaccharide lipid A derivatives containing a D-gluconolactone moiety have not been investigated. Thus, we decided to also synthesize Lipid X derivatives devoid of a phosphonate, yet containing the D-gluconolactone moiety (**21**, **22**, and **23**).

**Scheme 8 | *Rhizobium sin-1* lipid A.**



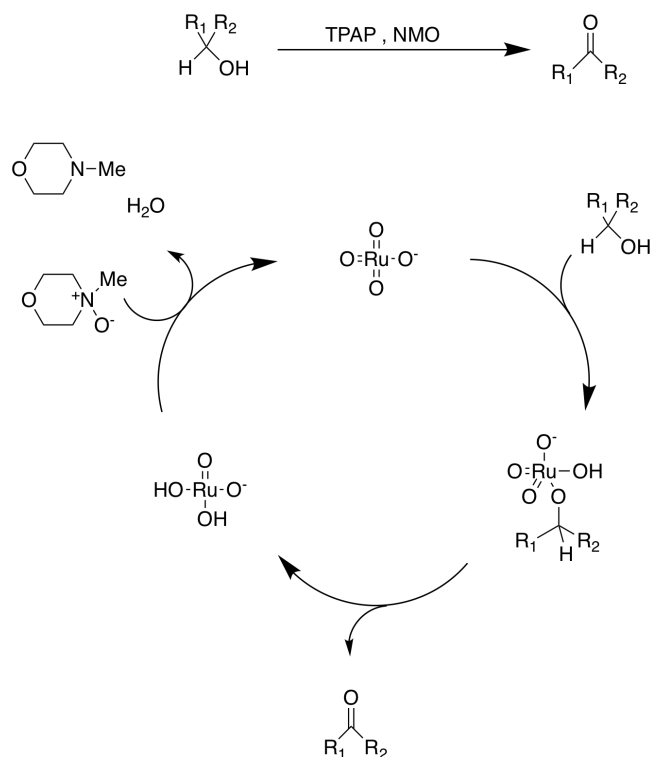
**24:** n = 10, 12, 14

**25:** R = C(=O)C<sub>27</sub>H<sub>55</sub>

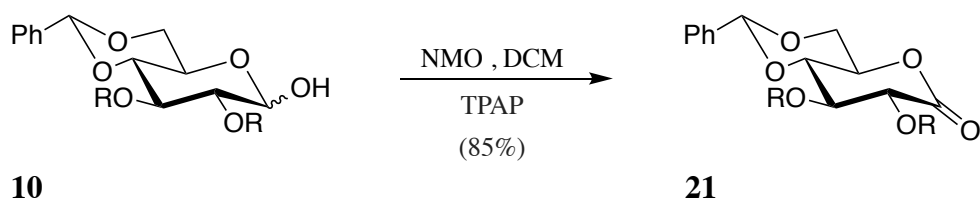
Oxidation of carbohydrates is a widely-utilized technique to attain derivatives with profoundly modified reactivity and character. Mono-oxidation of carbohydrates at the anomeric center produces aldonolactones with reactivity unlike that of the corresponding aldoses.

A facile synthetic technique we used to produce the desired Lipid X D-gluconolactone derivative (**21**) was by performing a Ley-Griffith oxidation to compound (**10**). This technique utilizes the ruthenium based oxidant tetrapropylammonium perruthenate  $N(C_3H_7)_4RuO_4$  (TPAP) with 1.5 equivalents of co-oxidant *N*-methylmorpholine *N*-oxide (NMO) in DCM as shown in **Scheme 9**. TPAP operates catalytically at room temperature and is devoid of explosive side products. When TPAP is used in the presence of NMO (**Scheme 10**), high yields are usually observed and this was supported in the formation of our D-gluconolactone derivative (**21**).

**Scheme 9 | Ley-Griffith oxidation mechanism.**



### Scheme 10 | Anomeric oxidation produces D-glucono- $\delta$ -lactone.

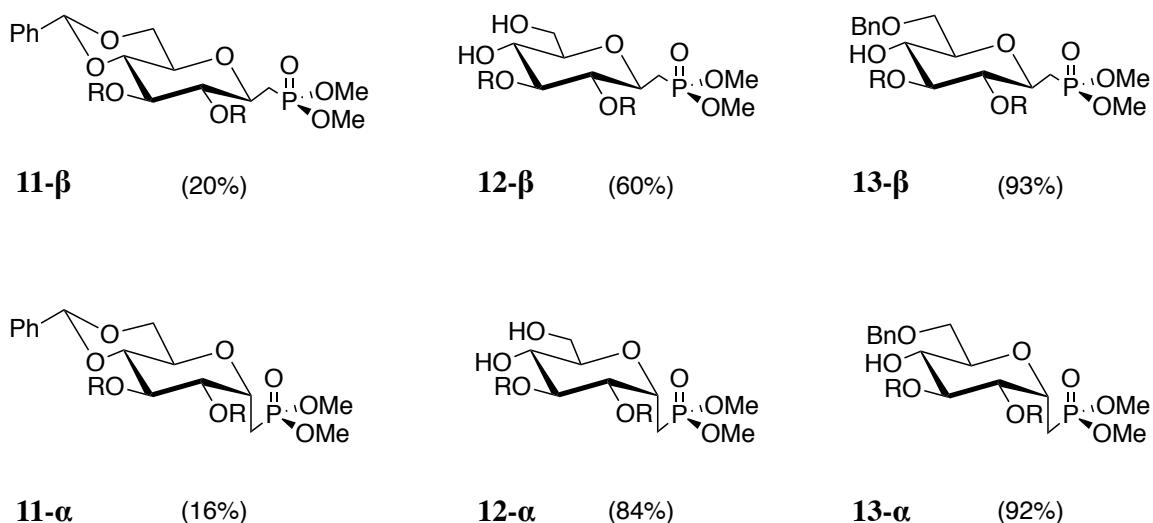


### 6. Chemistry of Horner-Emmons Reaction

This reaction makes use of phosphonate anions as the nucleophilic species. This methodology is applicable to the formation of C-glycosides (**11**) from sugars (**Scheme 11**). However, considering the intermediate  $\alpha$ ,  $\beta$ -unsaturated ester and the acidity of the proton at C-2, epimerization of the stereocenter is possible. Indeed, the reaction conditions that generated (**11**) did produce four diastereomers that were

### Scheme 11 | Generated phosphono-sugar mimetics

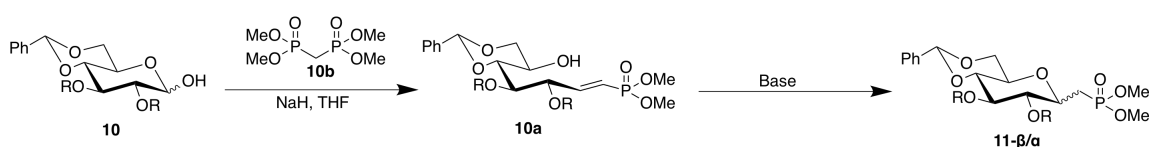
R = C<sub>14</sub>



isolated using preparatory reverse-phase HPLC. The byproducts with the "manno" configuration are not of biological significance, therefore were not subject to further chemistry for investigation. The anomeric ratio ( $\alpha:\beta$ ) varied from 3:2 to 1:1.

### Scheme 12 | Synthesis of phosphono-sugar mimetics

R = C<sub>14</sub>



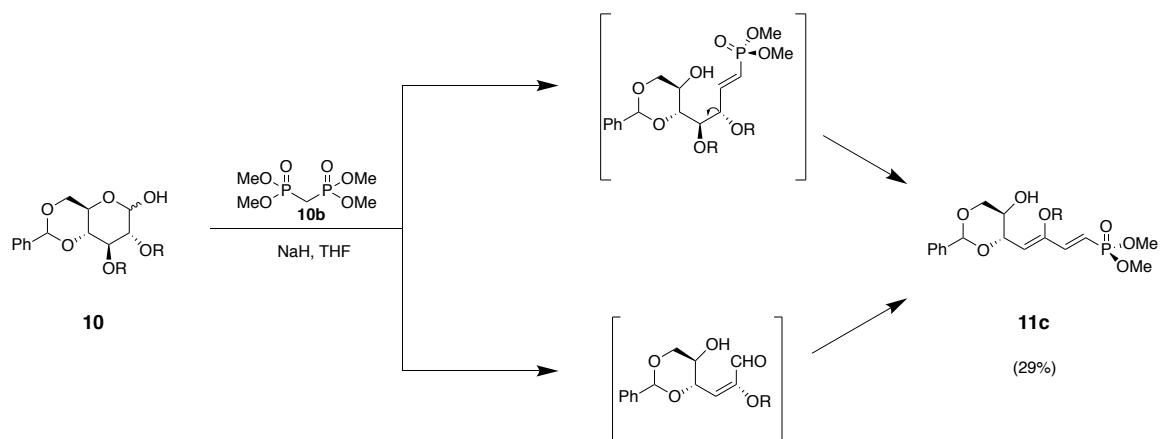
We unsuccessfully employed multiple strategies using traditional carbohydrate synthetic techniques to circumvent the generation of four diastereomers and to elicit regioselectivity in introduction of the phosphonate to C-1. A traditional approach to the methylene phosphonate analog (**Scheme 12**) involves reacting the benzylidene protected compound (**10**) with tetramethyl methylenediphosphonate (**10b**) to yield the vinyl phosphonate (**10a**) followed by base catalyzed cyclization to yield the phosphonate derivatives (**11-α/β**). In addition, the same mechanism that elicited epimerization at C-2 could account for the formation of the side product we isolated (**11c**) (460 mg, 29.2%), as depicted in **Scheme 13**. The elimination or reprotonation at C-2 produced



(**11c**) and contributed to the overall low yield (50.4%) of this reaction that generated four diastereomers of (**11**).

**Scheme 13 | Generation of side product 11c.**

R = C<sub>14</sub>



We applied the use of several bases including anhydrous Ba(OH)<sub>2</sub> in THF, KHMDS at -78°C in THF, DBU in THF, DIPEA in THF, and Cs<sub>2</sub>CO<sub>3</sub> in dry *i*-PrOH. Much to our surprise and without explanation, none of these bases generated the desired phosphonate product (**11-α/β**), except for NaH in THF. Crystallization of the 4,6-*O*-benzylidene β-glucoside (**11β**) was achieved, but not the α-configuration. Figure 14 is the depiction of the x-ray structure of (**11β**).

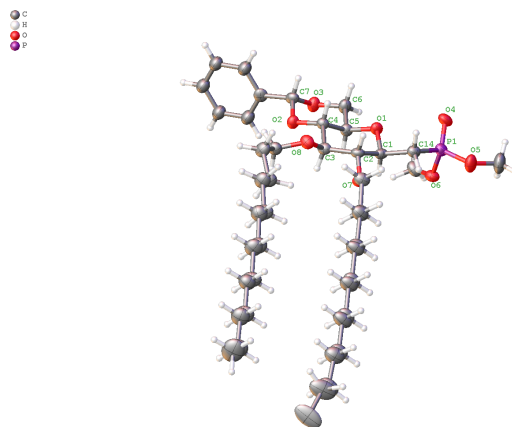


**Figure 14 | X-ray structure of 11.**

Only 4,6-*O*-benzylidene  $\beta$ -glucoside could be crystalized for x-ray crystallography.

At the reducing end of the sugar, the aldehyde is masked in form of a hemiacetal. However, the equilibrium between the hemiacetal and ring-opened form, especially considering ring strain of the 4,6-*O*-benzylidene, is highly favored towards the hemiacetal. Even so, the Wittig reaction can drive the equilibrium entirely to the ring-opened form, producing the newly formed olefin that can also be cyclized with addition of a base. To this end, we attempted to utilize a Wittig reagent that is readily available from Sigma Aldrich, diphenyl(triphenylphosphoranylidene)methylphosphonate  $\text{Ph}_3\text{P}=\text{CHPO}(\text{OBn})_2$ , to introduce a phosphonate to (**10**) with improved regioselectivity. This technique has been demonstrated to produce *C*-glycosylated phosphonate analogues with regioselectivity of the  $\alpha$ -anomer. Moreover, the anomeric

ratio of the product mixture is dependent upon the time exposure to the base. The Wittig method has been proven valuable for the formation of olefins from aldehydes and ketones using phosphorus ylides. Unfortunately, this method too did not work on our compound (**10**).

## 7. Biological Activity Assay

Compounds (**11 $\alpha$** , **11 $\beta$** , **12 $\alpha$** , **12 $\beta$** , **13 $\alpha$** , **13 $\beta$** , & **22**) were selected to be evaluated for anti-inflammatory potential against LPS-induced human acute monocytic leukemia (THP-1) cells. THP-1 cells provide an ideal system for studying inflammatory processes.<sup>88</sup> They serve as a model for peripheral monocytes/macrophages and their responsiveness to bacterial infection.<sup>88</sup> Unfortunately, benzylidene protected phosphono-sugar mimetics **11 $\alpha$**  and **11 $\beta$**  were not soluble in DMSO, therefore were not suitable for cell culture studies. The same result of insolubility was also observed for selectively ring-opened 6-O-benzyl ether compounds **13 $\alpha$**  and **13 $\beta$** . Albeit, they were seemingly more soluble than the completely protected benzylidene derivatives, more than likely due to the unveiled hydroxy at C-4. However, both complete benzylidene cleaved phosphono-mimetics **12 $\alpha$**  and **12 $\beta$**  and lactone derivative **22** were readily soluble in DMSO. Due to time constraints, we selected to evaluate the targeted and more biologically relevant  $\alpha$ -

anomer **12 $\alpha$**  and lactone derivative **22** by preincubating THP-1 cells with the compounds prior to cell stimulation with of *E. coli* LPS as outlined in experimentals. Modulation of TNF $\alpha$  production was analyzed *in vitro* and measured by ELISA.

## **8. Biological Activity**

THP-1 cells were stimulated with LPS in the presence of increasing concentrations of compounds **12 $\alpha$**  (Figure 14, red) and **22** (Figure 15, red) to test antagonistic activity. THP-1 cells were also treated with increasing concentrations of compounds **12 $\alpha$**  and **22** in the absence of LPS to examine agonistic activity (Figure 14 & 15, blue). Neither significantly demonstrated agonistic properties. The zero concentration of compound represents a control treatment of 100 ng/mL LPS and the same percentage of DMSO included with the compounds.

**Figure 14**

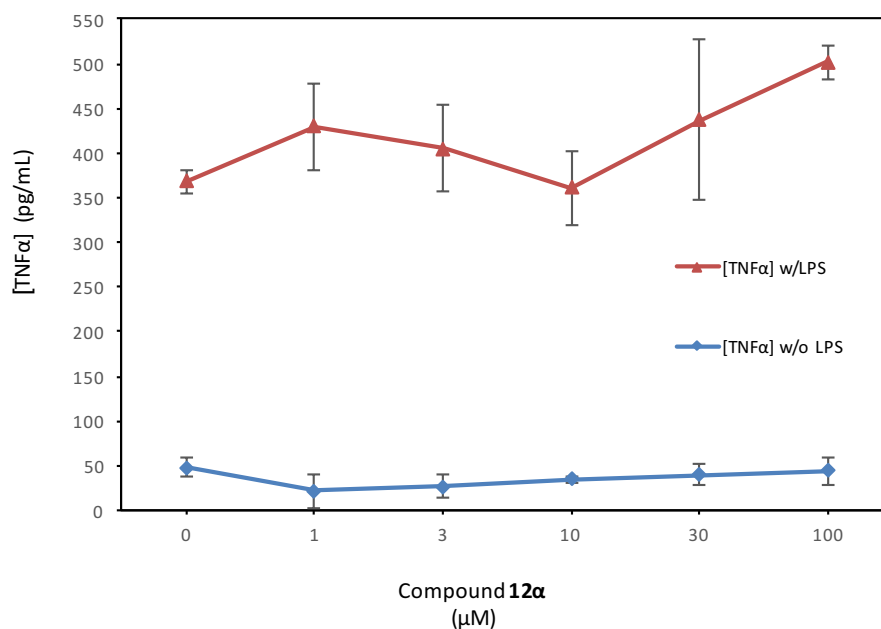


**Figure 14 | Effects to TNF $\alpha$  production in THP-1 cells in the presence of phosphono-sugar 12 $\alpha$ .**

Compound 12 $\alpha$  does not elicit antagonistic effects. THP-1 cells were treated as described in experimentals. Y-axis shows TNF $\alpha$  concentration in pg/mL. X-axis displays increasing concentrations of 12 $\alpha$  in the presence of LPS (red) and in absence of LPS (blue).

The targeted  $\alpha$ -phosphonate 12 $\alpha$  did not demonstrate antagonistic properties. However, compound 12 $\alpha$  appears to elicit slight synergistic effects by increasing TNF $\alpha$  production at 100  $\mu$ M. This finding may be attributed to cell toxicity.

**Figure 15**

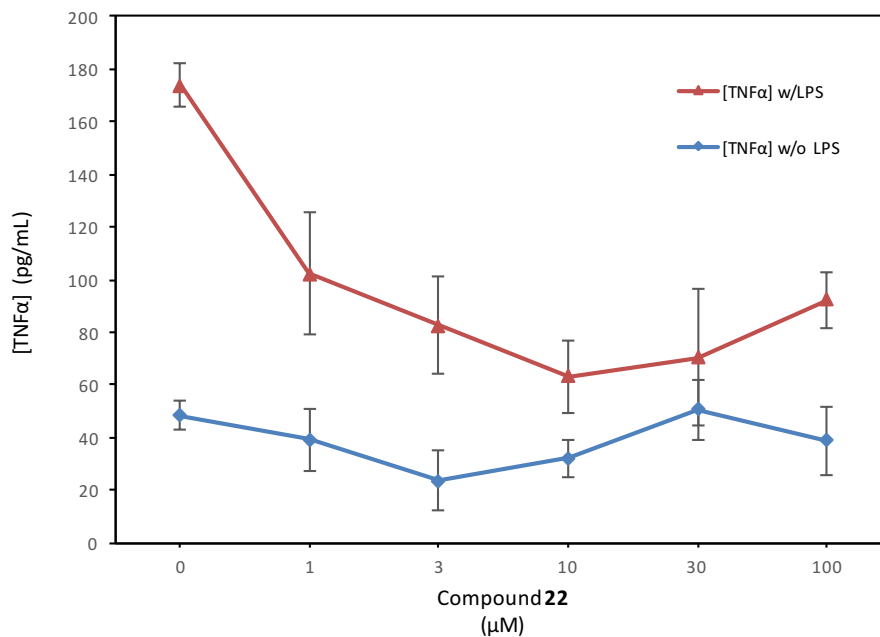


**Figure 15 | Effects to TNF $\alpha$  production in THP-1 cells in the presence of D-glucono- $\delta$ -lactone derivative 22.**

Compound 22 displays antagonistic properties. THP-1 cells were treated as described in experimentals. Y-axis shows TNF $\alpha$  concentration in pg/mL. X-axis displays increasing concentrations of 22 in the presence of LPS (red) and in absence of LPS (blue).

In contrast, D-glucono- $\delta$ -lactone derivative 22 did demonstrate antagonism by reducing TNF $\alpha$  production by 41% at the lowest tested concentration of 1  $\mu$ M. At concentrations of 3  $\mu$ M and 10  $\mu$ M TNF $\alpha$  production was further decreased by 52% and 64% respectively.

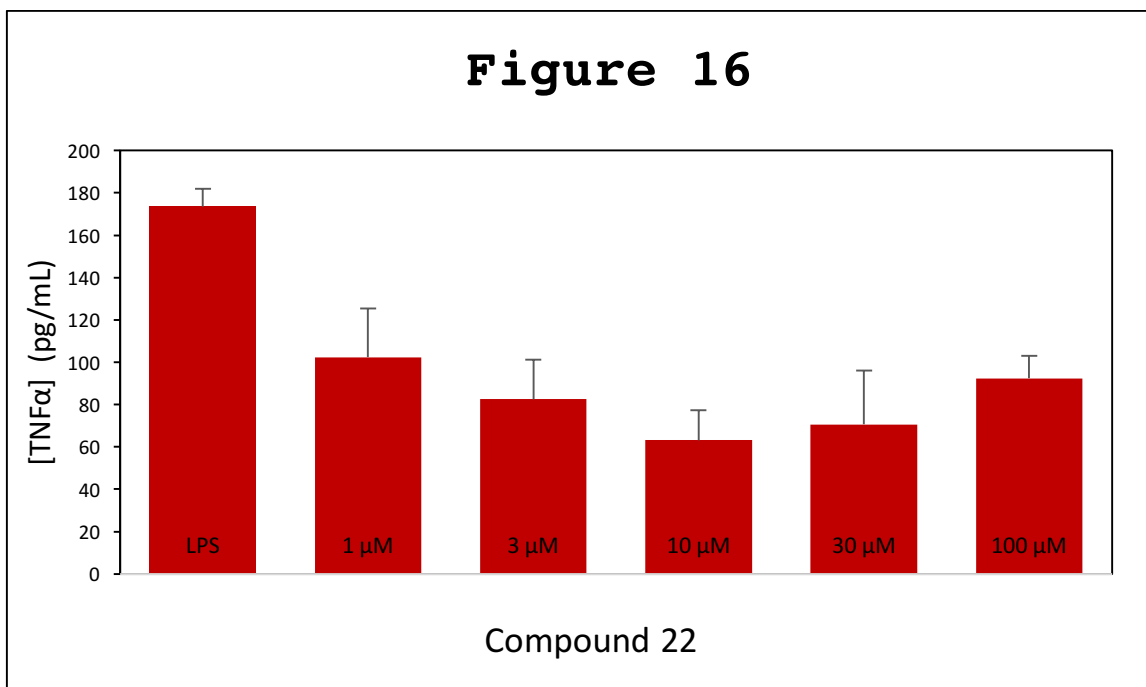


**Figure 16 | Compound 22 displays LPS antagonism.** THP-1 cells were treated as described in experimentals. Y-axis shows TNFα concentration in pg/mL. X-axis displays LPS without compound 22 (left) and going right are increasing concentrations of **22** in the presence of LPS. 41% inhibition is observed at 1 μM. Maximum inhibition of 64% was achieved at 10 μM.

#### **IV. Conclusion & Future Directions**

Sepsis is a clinical manifestation of a dysregulated and exaggerated inflammatory response to pathogenic microbes arising from our own innate immunity. Traditional interventions, which are geared towards attenuating the

symptoms of sepsis, have proved insufficient. This is supported by rising annual healthcare expenditures and high mortality rates in diagnosed patients. Moreover, antibiotic resistant strains of bacteria are ever-growing and are a cause for concern. Spearheaded efforts to enhance therapeutics by disrupting underlying mechanisms of immunopathogenesis will lead to improved patient outcomes.

The lipid A component of LPS causes immunopathogenesis by initiating TLR4-MD-2 receptor dimerization, consequently inducing the inflammatory pathway. Compounds that out-compete LPS would disrupt TLR4-MD-2 signal transduction and downregulate LPS signaling. Previously synthesized lipid A analogues demonstrate that subtle structural changes critically impact biological activity. Elucidating key chemical structure-activity relationships between lipid A variants will guide future explorations.

Our lipid A analogues were based upon the monosaccharide Lipid X with the aim to produce TLR4-MD-2 antagonist with more robust, simpler, and readily scalable chemical structures. Astute chemical modifications to substituents were aimed at improving bioavailability and solubility of lipid A analogues.

Synthesizing the C-glycosidic phosphono-sugar **12 $\alpha$**  produced a non-hydrolysable analogue that could circumvent



inactivation by host phosphatases. Unfortunately, **12 $\alpha$**  did not demonstrate LPS antagonism. Future attempts at synthesizing a phosphonate derivative should cleave the methyl protecting groups using TMSBr, which would yield the corresponding phosphonic acid of **12 $\alpha$** . In hind-sight, this modification could prove paramount in two ways. First, the anionic 1-phosphate of lipid A binds to positive patches on TLR4. The significance of this interaction has been established and is demonstrated by the previously mentioned mutagenesis studies and the attenuated endotoxicity of MPL (**4**). Second, the change in ionic character between the methyl protected and de-protected phosphonate substituent of **12 $\alpha$**  would potentially increase its solubility profile in aqueous media.

D-glucono- $\delta$ -lactone derivative **22** evaded the solubility issues compounds **11 $\alpha$** , **11 $\beta$** , **12 $\beta$** , **13 $\alpha$** , and **13 $\beta$**  encountered from their inherent amphipathic nature. More importantly, compound **22** demonstrated LPS antagonism in monocytic THP-1 cells, representing the first lactone monosaccharide *R. sin-1* lipid A derivative to do so. Albeit, monosaccharide **22** does not inhibit LPS signaling as much as some disaccharide compounds like Eritoran (**3**). However, the comparative ease of synthesis could outweigh their differences of inhibition.

Overall, this embodiment of work provides new information regarding monosaccharide-based lipid A analogues.

Results from the studies herein provide a scientific basis for future investigations of lipid A antagonist, with added implications of inhibiting the adverse effects of septicemia. It is my hope that this work reveals structural insights of antagonistic properties to guide future explorations that ultimately lead to improved patient outcomes.

## **V. Experimentals**

### **1. General Procedures**

Glassware used for all experiments were oven-dried and all reactions were carried out under argon atmosphere unless otherwise mentioned. All reaction solvents were purified prior to use:  $\text{CH}_2\text{Cl}_2$  was dried by distillation over calcium hydride; THF was distilled over sodium. Reagent grade DMF and HPLC grade MeOH was obtained from Sigma-Aldrich and used without further purification.

NMR spectra were recorded at 600 MHz or 300 MHz. Chemical shifts ( $\delta$ ) for  $^1\text{H}$  and  $^{13}\text{C}$  spectra are expressed in ppm relative to internal standard ( $\text{CDCl}_3$ : 7.26 for  $^1\text{H}$  and 77.23 for  $^{13}\text{C}$ ). Chemical shifts for  $^{31}\text{P}$  were referenced with phosphoric acid

and then back calculated. Signals were abbreviated as s, singlet; d, doublet; dd, doublet of doublets; t, triplet; q, quartet; m, multiplet. Thin layer chromatography (TLC) was carried out with pre-coated Merck F254 silica gel plates. Flash chromatography (FC) was carried out with Macherey-Nagel silica gel 60-230 mesh. Automated preparative chromatography was performed using a Biotage Isolera Prime or reverse phase C<sub>18</sub> HPLC preparatory system.

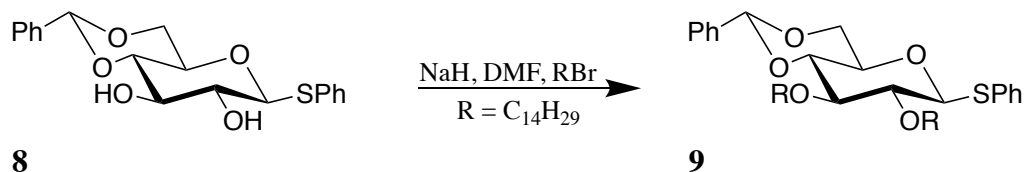
## **2. General Procedure for selective C4 ring opening of 4,6-O-benzylidene**

A stirred solution of 4,6-O-Benzylidene (0.1 mmol) in dry THF (0.66 mL) containing 4 Å molecular sieves was added NaCNBH<sub>3</sub> (13.3 eq.). The reaction mixture was stirred for 5 min. and subsequent addition of 2 N HCl/Et<sub>2</sub>O (13.3 eq.) was added in portions using a syringe over 10 min. The reaction was monitored by TLC until complete disappearance of starting material. The reaction mixture was then filtered through celite, diluted with DCM, washed with H<sub>2</sub>O (x1), HCO<sub>3</sub><sup>-</sup> (x1), H<sub>2</sub>O (x1), dried over Na<sub>2</sub>SO<sub>4</sub> and concentrated *in vacuo*. The residue was separated by preparative HPLC.

### 3. General Procedure for C6/C4 complete ring cleavage of 4,6-*O*-benzylidene

4,6-*O*-Benzylidene (0.05 mmol) was dissolved in TFA and DCM (15% TFA in DCM, 0.7 mL) and stirred for 20 min. One drop of H<sub>2</sub>O was added and the reaction was stirred for 1 h. Reaction was monitored by TLC until complete and then concentrated *in vacuo*. The residue was azeotroped with toluene (1 mL x 4) and finally concentrated *in vacuo*. The residue was separated by preparative HPLC.

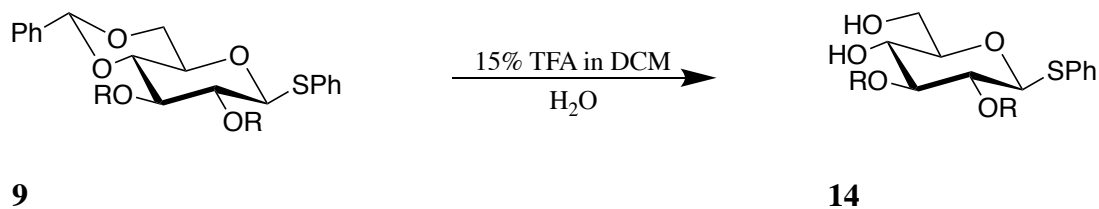
#### Synthesis of 4,6-*O*-benzylidene-2,3-*O*-tetradecane- $\beta$ -thiophenol-D-glucopyranose (**9**)



A stirred solution of 4,6-*O*-benzylidene-2,3-diol- $\beta$ -thiophenol-D-glucopyranose<sup>87</sup> (**8**) (9.15 g, 25.25 mmol) in dry DMF (18 mL) containing 4 Å molecular sieves was cooled to 0°C. A suspension of NaH (1.4g, 55.55 mmol) mixed in dry THF (12 mL) was added portion wise over 15 minutes. The reaction mixture was allowed to warm up to 40°C and was stirred for 30 minutes. A catalytic amount of tetra-*N*-butylammonium iodide (0.933g, 2.52 mmol) was added to the mixture immediately

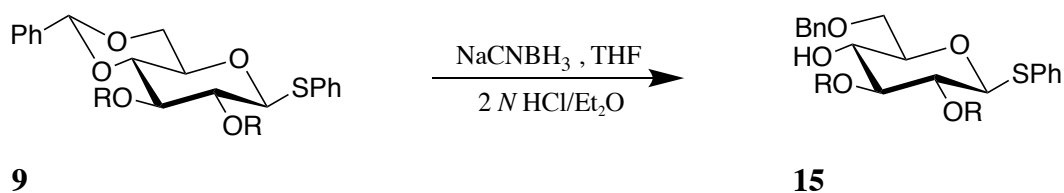
followed by dropwise addition of bromo-tetradecane (15.4 g, 55.55 mmol) over 30 minutes. Reaction was monitored by TLC. After 24 hours, no further conversion of the starting material could be detected. The reaction mixture was cooled to 0°C, diluted with CH<sub>2</sub>Cl<sub>2</sub> (30 mL), quenched with NH<sub>4</sub>Cl, and washed with H<sub>2</sub>O (x 3). The organic phase was dried over Na<sub>2</sub>SO<sub>4</sub>, filtered and concentrated *in vacuo*. The residue was purified by column chromatography on silica gel (ethyl acetate-hexane gradient elution) to afford the title compound **(9)** (14.8 g, 78%) as a white solid. **(9)**: <sup>1</sup>H NMR (600 MHz Chloroform-*d*) δ 7.55 – 7.24 (m, 10H), 5.53 (s, 1H), 4.65 (d, *J* = 9.8 Hz, 1H), 4.34 (dd, *J* = 10.5, 5.0 Hz, 1H), 3.84 (m, 1H), 3.76 (m, 3H), 3.68 (m, 1H), 3.53 (m, 2H), 3.44 – 3.36 (m, 1H), 3.21 (dd, *J* = 9.7, 8.0 Hz, 1H), 1.66 – 1.50 (m, 10H), 1.42 – 1.18 (m, 38H), 0.88 (t, *J* = 7.0 Hz, 6H).

**Synthesis of 4,6-diol-2,3-O-tetradecane-β-thiophenol-D-glucopyranose (14)**



Compound (**14**) was synthesized from (**9**, 100 mg, 0.133 mmol) using the general procedure 3 above (yield, 68.5 mg, 77%). (**14**):  $^1\text{H}$  NMR (600 MHz, Chloroform-*d*)  $\delta$  7.53 – 7.41 (m, 2H), 7.33 – 7.23 (m, 3H), 4.62 (d,  $J = 9.7$  Hz, 1H), 3.93 – 3.86 (m, 2H), 3.83 – 3.72 (m, 2H), 3.70 – 3.62 (m, 2H), 3.52 – 3.46 (m, 1H), 3.38 – 3.33 (m, 1H), 3.26 (t,  $J = 8.9$  Hz, 1H), 3.16 (t, 1H), 2.46 (s, 1H), 2.04 (s, 1H), 1.65 – 1.55 (m, 4H), 1.48 – 1.05 (m, 44H), 0.88 (t,  $J = 7.0$  Hz, 6H).  $^{13}\text{C}$  NMR (151 MHz, Chloroform-*d*)  $\delta$  133.97, 131.68, 129.11, 127.64, 107.49, 107.48, 87.98, 86.36, 81.20, 79.16, 73.97, 73.63, 71.73, 70.65, 63.03, 32.08, 30.61, 30.51, 29.87, 29.85, 29.83, 29.79, 29.72, 29.71, 29.53, 26.31, 26.28, 22.85.

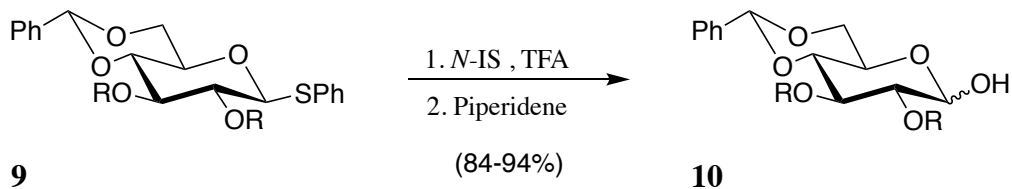
**Synthesis of 6-O-benzyl-4-hydroxy-2,3-O-tetradecane- $\beta$ -thiophenol-D-glucopyranose (**15**)**



Compound (**15**) was synthesized from (**9**, 100 mg, 0.133 mmol) using the general procedure 2 above (yield, 84.58 mg, 84%). (**15**):  $^1\text{H}$  NMR (300 MHz, Chloroform-*d*)  $\delta$  7.52 – 7.38 (m, 2H), 7.29 – 7.14 (m, 8H), 4.50 (s, 2H), 3.83 – 3.53 (m, 6H), 3.51

- 3.33 (m, 2H), 3.26 - 3.01 (m, 2H), 2.60 (s, 1H), 1.61 - 1.46 (m, 5H), 1.31 - 1.14 (m, 44H), 0.82 (t,  $J = 6.5$  Hz, 6H).

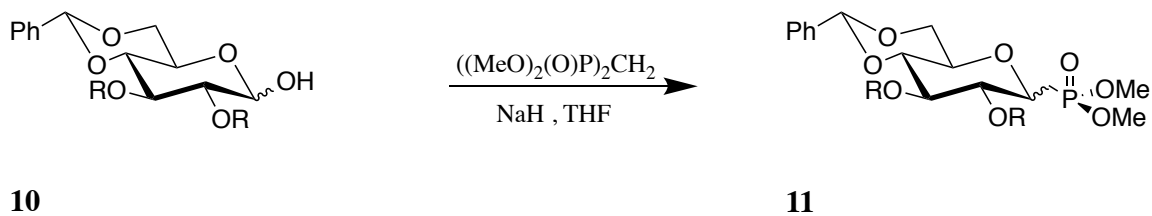
**Synthesis of 4,6-O-benzylidene-2,3-O-tetradecane- $\alpha/\beta$ -D-glucopyranose (10)**



Thio-glucoside (**9**) (1.022 g, 1.357 mmol) was dissolved in  $\text{CH}_2\text{Cl}_2$  (14 mL) and the reaction mixture was stirred and cooled to  $0^\circ\text{C}$ . NIS (335.83 mg, 1.493 mmol 1.1 equiv.) and TFA (114.30  $\mu\text{L}$ , 1.493 mmol, 1.1 equiv.) were added. The reaction was allowed to warm to room temp. After 1 h, the reaction mixture was cooled to  $0^\circ\text{C}$ , and piperidine (402.12  $\mu\text{L}$ , 4.071 mmol, 3 equiv.) was added. After 30 min, TLC analysis showed total conversion of the anomeric trifluoroacetate into a compound with a lower  $R_f$  (DCM/Hexanes 5:3, v/v,  $R_f$  0.10). The reaction mixture was quenched by the subsequent addition of triethylamine (the reaction turned from dark red to yellow) and  $\text{Na}_2\text{S}_2\text{O}_3$  (aq., 20%, the yellow reaction mixture turned colorless). The reaction mixture was diluted with  $\text{CH}_2\text{Cl}_2$ , washed with  $\text{H}_2\text{O}$ , dried with  $\text{Na}_2\text{SO}_4$ , filtered through celite, and concentrated in vacuo. Flash chromatography

(EtOAc:Hexanes 1.25:10, v/v, isocratic) afforded hemiacetal (**10**) as an anomeric mixture ( $\alpha/\beta$  1:1, 760.3 mg, 84%) as a white solid. (**10**):  $^1\text{H}$  NMR (300 MHz, Chloroform-*d*)  $\delta$  7.53 - 7.43 (m, 2H), 7.42 - 7.30 (m, 3H), 5.54 (s, 1H), 5.30 (d,  $J$  = 3.8 Hz, 0.5H), 4.73 (d,  $J$  = 7.7 Hz, 0.5H), 4.36 - 4.27 (m, 1H), 4.12 - 3.94 (m, 1H), 3.86 - 3.75 (m, 2H), 3.73 - 3.63 (m, 3H), 3.61 - 3.44 (m, 2H), 3.43 - 3.34 (m, 1H), 3.12 (t,  $J$  = 8.0 Hz, 1H), 1.57 (s, 10H), 1.35 - 1.18 (m, 38H), 0.88 (t,  $J$  = 6.5 Hz, 6H).

**Synthesis of 4,6-O-benzylidene-2,3-O-tetradecane- $\alpha/\beta$ -D-methylene-dimethyl-phosphono-glucoside (**11**)**



A stirred solution of dry  $\text{CH}_2\text{Cl}_2$ :THF (12 mL, 1:3 respectively) and NaH (95% oil dispersion, 106.95 mg, 4.282 mmol, 1.5 eq.) was cooled to  $0^\circ\text{C}$ .  $((\text{MeO})_2(\text{O})\text{P})_2\text{CH}_2$  (633.6  $\mu\text{L}$ , 3.426 mmol, 1.2 eq.) was added portion wise with a syringe over 15 minutes. The reaction mixture was allowed to warm up to room temperature and was stirred for 30 minutes. The reaction mixture was again cooled to  $0^\circ\text{C}$  and (**10**) (1.877 g, 2.855 mmol) in dry  $\text{CH}_2\text{Cl}_2$ :THF (4 mL, 1:3 respectively) was added dropwise



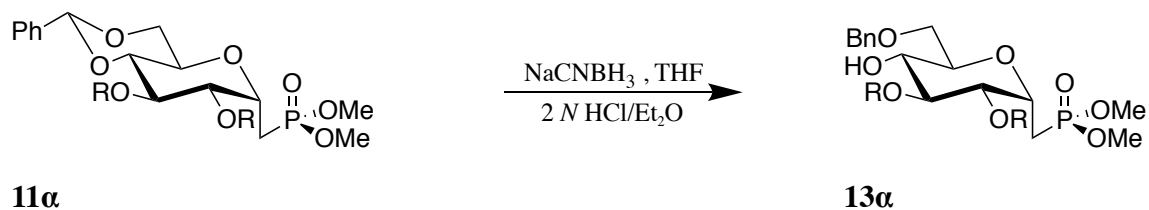
via an addition funnel over 30 mins. The reaction mixture was allowed to warm up to room temperature and was monitored via HPLC. After 23 h, the reaction mixture was cooled to 0°C, quenched with NH<sub>4</sub>Cl, diluted with CH<sub>2</sub>Cl<sub>2</sub>, washed with H<sub>2</sub>O (x1), HCO<sub>3</sub><sup>-</sup> (aq. satd., x1), H<sub>2</sub>O (x1), dried with Na<sub>2</sub>SO<sub>4</sub>, filtered through celite, and concentrated in vacuo. Flash chromatography (EtOAc:Hexanes 1:4, v/v, isocratic) afforded **(11)** (1.104 g, 50.4%) as a white solid mixture of four diastereomers. The mixture was separated by preparative HPLC to afford; (11c-manno, 24.34 mg, 1.11%, R<sub>f</sub> 4.331,); (7a-9a, 351.11 mg, 16.03%, R<sub>f</sub> 5.875); (11d-manno, 31.56 mg, 1.44%, R<sub>f</sub> 8.182); (15a-20a, 427.32 mg, 19.51%, R<sub>f</sub> 8.353) white solids.

**(11c-manno)**: <sup>1</sup>H NMR (600 MHz, Chloroform-*d*) δ 7.50 - 7.43 (m, 2H), 7.38 - 7.28 (m, 3H), 5.60 (s, 1H), 4.47 (q, *J* = 7.7 Hz, 1H), 4.20 (dd, *J* = 10.2, 4.6 Hz, 1H), 4.10 (t, *J* = 9.6 Hz, 1H), 3.85 - 3.54 (m, 14H), 2.31 - 2.22 (m, 1H), 2.13 - 2.04 (m, 1H), 1.66 - 1.55 (m, 5H), 1.38 - 1.22 (m, 45H), 0.88 (t, *J* = 6.7 Hz, 6H). <sup>13</sup>C NMR (151 MHz, Chloroform-*d*) δ 137.74, 128.87, 128.26, 126.10, 101.40, 79.06, 78.39, 78.32, 76.17, 72.64, 71.99, 71.29, 69.07, 66.22, 52.90, 52.86, 52.68, 52.64, 32.07, 30.18, 29.99, 29.86, 29.84, 29.82, 29.69, 29.66, 29.52, 26.59, 26.27, 26.18, 25.66, 22.84, 14.27. <sup>31</sup>P NMR (243 MHz, Chloroform-*d*) δ 30.32. **(11α)**: <sup>1</sup>H NMR (600 MHz, Chloroform-*d*) δ 7.52 - 7.44 (m, 2H), 7.39 - 7.29 (m, 3H),

5.58 (s, 1H), 4.24 (dd,  $J = 10.3, 4.9$  Hz, 1H), 4.03 - 3.95 (m, 2H), 3.92 - 3.87 (m, 1H), 3.81 (t,  $J = 10.3$  Hz, 1H), 3.78 - 3.69 (m, 7H), 3.63 - 3.58 (m, 1H), 3.56 - 3.48 (m, 2H), 3.44 - 3.39 (m, 1H), 2.20 (ddd,  $J = 18.4, 6.3, 4.8$  Hz, 2H), 1.64 - 1.56 (m, 4H), 1.42 - 1.19 (m, 44H), 0.88 (t,  $J = 7.0$  Hz, 6H).  $^{13}\text{C}$  NMR (151 MHz, Chloroform-*d*)  $\delta$  137.77, 128.88, 128.25, 126.15, 101.38, 81.10, 78.77, 74.84, 74.41, 72.01, 71.71, 68.59, 52.87, 52.83, 52.29, 52.24, 32.08, 30.44, 30.28, 29.88, 29.85, 29.83, 29.72, 29.65, 29.53, 27.95, 27.01, 26.28, 26.25, 22.85, 14.28.  $^{31}\text{P}$  NMR (243 MHz, Chloroform-*d*)  $\delta$  31.67. **(11d-manno)**:  $^1\text{H}$  NMR (600 MHz, Chloroform-*d*)  $\delta$  7.50 - 7.44 (m, 2H), 7.39 - 7.32 (m, 3H), 5.53 (s, 1H), 4.57 - 4.51 (m, 1H), 4.25 (dd,  $J = 9.8, 4.3$  Hz, 1H), 3.80 - 3.70 (m, 7H), 3.69 - 3.60 (m, 4H), 3.58 - 3.52 (m, 2H), 3.51 - 3.48 (m, 1H), 3.47 - 3.44 (m, 1H), 2.28 - 2.18 (m, 2H), 1.65 (s, 1H), 1.59 - 1.51 (m, 4H), 1.37 - 1.22 (m, 44H), 0.88 (t,  $J = 7.0$  Hz, 6H).  $^{13}\text{C}$  NMR (151 MHz, Chloroform-*d*)  $\delta$  137.54, 128.99, 128.32, 126.10, 101.27, 82.31, 79.66, 79.57, 78.68, 73.33, 72.26, 71.14, 71.10, 69.45, 64.34, 52.60, 52.56, 52.52, 32.08, 30.47, 30.27, 29.87, 29.84, 29.82, 29.80, 29.71, 29.66, 29.53, 26.29, 26.26, 22.85, 14.28, 1.17.  $^{31}\text{P}$  NMR (243 MHz, Chloroform-*d*)  $\delta$  32.76. **(11 $\beta$ )**:  $^1\text{H}$  NMR (600 MHz, Chloroform-*d*)  $\delta$  7.49 - 7.45 (m, 2H), 7.39 - 7.32 (m, 3H), 5.52 (s, 1H), 4.31 (dd,  $J =$

10.3, 4.9 Hz, 1H), 3.91 - 3.85 (m, 2H), 3.76 - 3.71 (m, 6H), 3.70 - 3.68 (m, 1H), 3.68 - 3.66 (m, 1H), 3.66 - 3.63 (m, 1H), 3.55 - 3.48 (m, 3H), 3.46 - 3.42 (m, 1H), 3.05 (t, 1H), 2.40 - 2.33 (m, 1H), 1.97 - 1.90 (m, 1H), 1.59 - 1.54 (m, 4H), 1.31 - 1.20 (m, 44H), 0.88 (t,  $J = 7.0$  Hz, 6H).  $^{13}\text{C}$  NMR (151 MHz, Chloroform-*d*)  $\delta$  137.54, 129.01, 128.34, 126.12, 101.23, 83.19, 82.41, 82.32, 82.17, 75.39, 73.94, 73.47, 70.64, 68.86, 52.67, 52.31, 32.09, 30.58, 30.54, 29.87, 29.83, 29.72, 29.71, 29.53, 26.34, 26.32, 22.85, 14.29.  $^{31}\text{P}$  NMR (243 MHz, Chloroform-*d*)  $\delta$  31.83.

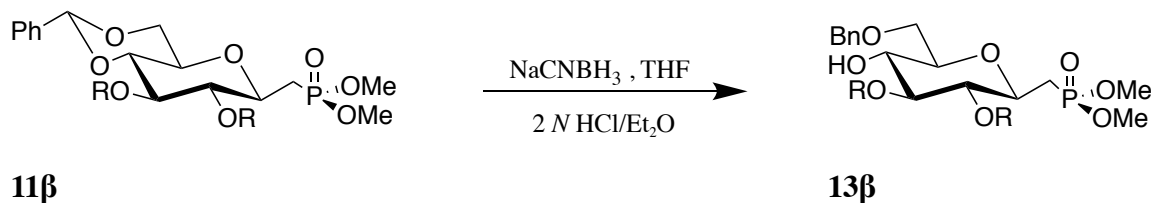
**Synthesis of 6-O-benzyl-4-hydroxy-2,3-O-tetradecane- $\alpha$ -D-methylene-dimethyl-phosphono-glucoside (13 $\alpha$ )**



Compound (**13 $\alpha$** ) was synthesized from (**11 $\alpha$** , 100 mg, 0.1304 mmol) using the general procedure 2 above (yield, 92.27 mg, 92%). (**13 $\alpha$** ):  $^1\text{H}$  NMR (300 MHz, Chloroform-*d*)  $\delta$  7.35 - 7.26 (m, 5H), 4.89 (d,  $J = 10.8$  Hz, 1H), 4.60 (d,  $J = 11.0$  Hz, 1H), 3.98 - 3.87 (m, 1H), 3.84 - 3.60 (m, 10H), 3.52 (t,  $J = 7.9$  Hz, 2H), 3.45 - 3.38 (m, 1H), 3.38 - 3.27 (m, 1H), 2.28 - 2.07 (m,

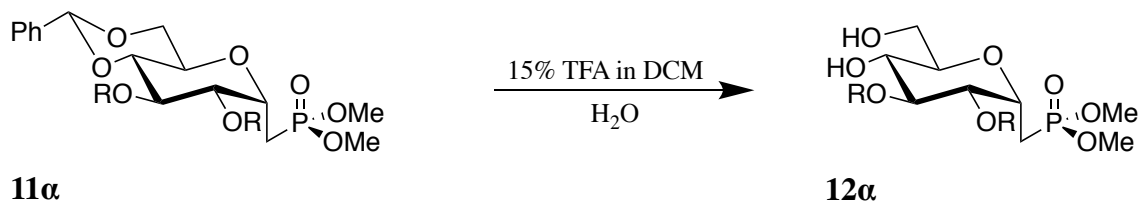
2H), 1.71 - 1.51 (m, 9H), 1.39 - 1.18 (m, 42H), 0.88 (t,  $J = 6.5$  Hz, 6H).

**Synthesis of 6-O-benzyl-4-hydroxy-2,3-O-tetradecane- $\beta$ -D-methylene-dimethyl-phosphono-glucoside (13 $\beta$ )**



Compound (**13 $\beta$** ) was synthesized from (**11 $\beta$** , 35.6 mg, 0.0464 mmol) using the general procedure 2 above (yield, 32.8 mg, 92%). (**13 $\beta$** ):  $^1H$  NMR (600 MHz, Chloroform-*d*)  $\delta$  7.38 - 7.23 (m, 5H), 4.58 - 4.52 (m, 2H), 3.83 - 3.75 (m, 2H), 3.75 - 3.65 (m, 8H), 3.65 - 3.35 (m, 5H), 3.22 (t,  $J = 8.9$  Hz, 1H), 2.96 (t,  $J = 9.2$  Hz, 1H), 2.65 (s, 1H), 2.36 - 2.29 (m, 1H), 1.96 - 1.89 (m, 1H), 1.78 - 1.61 (m, 2H), 1.61 - 1.48 (m, 4H), 1.48 - 1.07 (m, 42H), 0.87 (t,  $J = 7.0$  Hz, 6H).  $^{13}C$  NMR (151 MHz, Chloroform-*d*)  $\delta$  137.93, 128.54, 127.90, 86.43, 86.41, 82.18, 82.09, 78.03, 74.81, 74.76, 73.73, 73.50, 72.12, 70.45, 52.71, 52.67, 52.28, 52.24, 32.08, 30.65, 30.55, 29.87, 29.85, 29.82, 29.80, 29.73, 29.72, 29.52, 28.54, 27.59, 26.31, 22.85, 14.28.  $^{31}P$  NMR (243 MHz, Chloroform-*d*)  $\delta$  32.20.

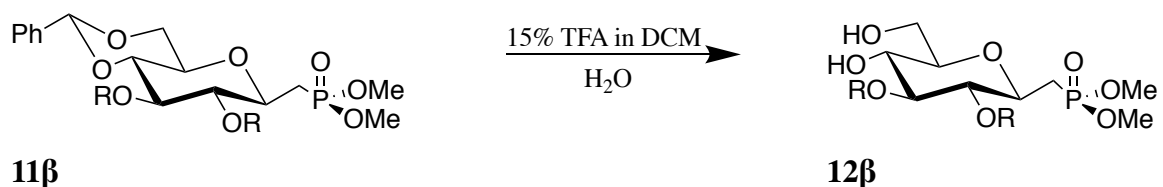
**Synthesis of 4,6-diol-2,3-O-tetradecane- $\alpha$ -D-methylene-  
dimethyl-phosphono-glucoside (**12 $\alpha$** )**



Compound (**12 $\alpha$** ) was synthesized from (**11 $\alpha$** , 44 mg, 0.0574 mmol) using the general procedure 3 above (yield, 32.7 mg, 84%).

(**12 $\alpha$** ):  $^1\text{H}$  NMR (600 MHz, Chloroform-*d*)  $\delta$  3.91 – 3.58 (m, 13H), 3.47 (q,  $J$  = 6.9 Hz, 1H), 3.43 – 3.39 (m, 1H), 3.37 – 3.32 (m, 1H), 3.24 (dd,  $J$  = 9.4, 2.4 Hz, 1H), 2.49 (s, 1H), 2.27 – 2.21 (m, 1H), 2.15 – 2.09 (m, 1H), 1.84 (s, 1H), 1.63 – 1.54 (m, 4H), 1.44 – 1.09 (m, 44H), 0.87 (t,  $J$  = 7.0 Hz, 6H).  $^{13}\text{C}$  NMR (151 MHz, Chloroform-*d*)  $\delta$  84.76, 79.77, 75.37, 75.31, 73.68, 73.65, 70.24, 67.51, 63.28, 52.77, 52.72, 52.50, 52.46, 32.07, 30.41, 30.11, 29.85, 29.83, 29.81, 29.80, 29.77, 29.76, 29.65, 29.51, 28.03, 27.09, 26.29, 26.22, 22.84, 14.27.  $^{31}\text{P}$  NMR (243 MHz, Chloroform-*d*)  $\delta$  31.84.

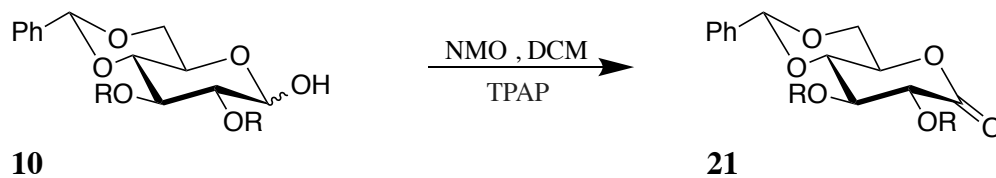
**Synthesis of 4,6-diol-2,3-O-tetradecane- $\beta$ -D-methylene-  
dimethyl-phosphono-glucoside (**12 $\beta$** )**



Compound (**12 $\beta$** ) was synthesized from (**11 $\beta$** , 39 mg, 0.0508 mmol) using the general procedure 3 above (yield, 20.8 mg, 60%).

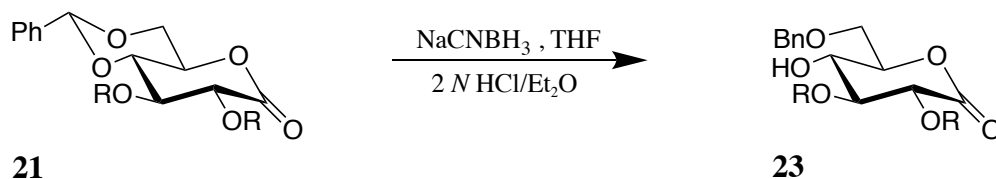
(**12 $\beta$** ):  $^1\text{H}$  NMR (600 MHz, Chloroform-*d*)  $\delta$  3.84 – 3.69 (m, 10H), 3.58 – 3.44 (m, 4H), 3.33 (dd,  $J = 7.4, 4.7$  Hz, 1H), 3.23 (t,  $J = 9.0$  Hz, 1H), 2.95 (t,  $J = 9.2$  Hz, 1H), 2.35 – 2.28 (m, 1H), 2.00 – 1.91 (m, 2H), 1.65 – 1.47 (m, 5H), 1.38 – 1.06 (m, 44H), 0.93 – 0.79 (m, 6H).  $^{13}\text{C}$  NMR (151 MHz, Chloroform-*d*)  $\delta$  86.43, 86.41, 82.62, 82.53, 79.71, 74.57, 74.52, 73.79, 73.55, 71.07, 62.62, 52.74, 52.69, 52.61, 52.57, 32.07, 30.65, 30.56, 29.86, 29.85, 29.82, 29.81, 29.79, 29.74, 29.72, 29.52, 28.63, 27.68, 26.31, 26.30, 22.84, 14.27.  $^{31}\text{P}$  NMR (243 MHz, Chloroform-*d*)  $\delta$  32.47.

**Synthesis of 4,6-O-benzylidene-2,3-O-tetradecane-D-glucono- $\delta$ -lactone (21)**



A mixture of 4,6-O-benzylidene-2,3-O-tetradecane- $\alpha/\beta$ -D-glucopyranose (**10**) (491.2 mg, 0.743 mmol), tetrapropylammonium perruthenate  $\text{N}(\text{C}_3\text{H}_7)_4\text{RuO}_4$  (26.11 mg, 0.0743 mmol), *N*-methyl-*N*-morpholine oxide (130.56 mg, 1.115 mmol) and MS, 4 Å (0.57 g) in  $\text{CH}_2\text{Cl}_2$  (19 mL) was stirred at room temperature for 2 h. Upon reaction completion, the mixture was diluted with DCM (50 mL) and washed with 5% sodium sulfite in brine, brine, and copper sulfate (10 mL, each). The combined organic extract was dried over  $\text{Na}_2\text{SO}_4$ , filtered through Celite, and concentrated *in vacuo*, and the concentrated residue was purified by silica column chromatography to afford (**21**) the title compound (416.49 mg, 85%) as a white solid. (**21**):  $^1\text{H}$  NMR (300 MHz, Chloroform-*d*)  $\delta$  7.53 – 7.45 (m, 2H), 7.42 – 7.33 (m, 3H), 5.58 (s, 1H), 4.56 – 4.43 (m, 2H), 3.98 – 3.91 (m, 1H), 3.84 – 3.76 (m, 3H), 3.75 – 3.55 (m, 4H), 1.62 – 1.55 (m, 4H), 1.25 (s, 44H), 0.88 (t,  $J = 7.0, 5.9$  Hz, 6H).

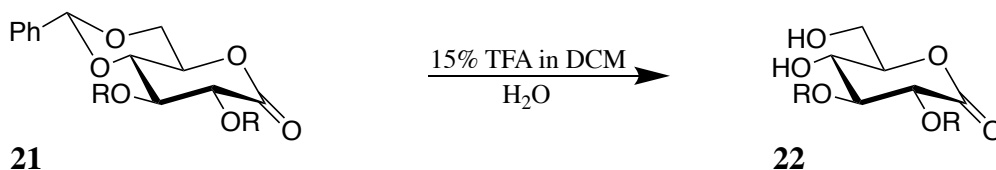
**Synthesis of 6-O-benzyl-4-hydroxy-2,3-O-tetradecane-D-glucono- $\delta$ -lactone (23)**



Compound (**23**) was synthesized from (**21**, 100 mg, 0.1517 mmol) using the general procedure 2 above (yield, 78.66 mg, 78%).

(**23**):  $^1\text{H NMR}$  (300 MHz, Chloroform-*d*)  $\delta$  7.28 – 7.13 (m, 5H), 4.46 (d,  $J = 2.0$  Hz, 2H), 3.73 – 3.38 (m, 11H), 2.81 (s, 1H), 2.53 (s, 1H), 1.54 – 1.38 (m, 4H), 1.14 (s, 42H), 0.76 (t,  $J = 6.0$  Hz, 6H).

**Synthesis of 4,6-diol-2,3-O-tetradecane-D-glucono- $\delta$ -lactone (22)**



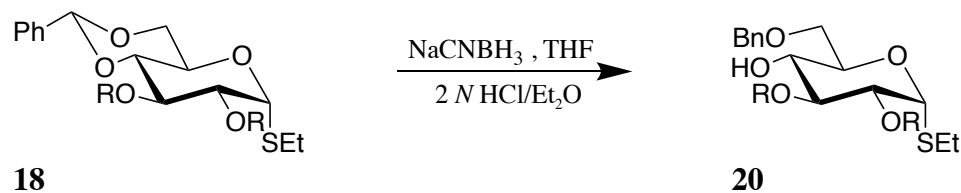
Compound (**22**) was synthesized from (**21**, 50 mg, 0.07587 mmol) using the general procedure 3 above (yield, 35.08 mg, 81%).

(**22**):  $^1\text{H NMR}$  (300 MHz, Chloroform-*d*)  $\delta$  4.60 – 4.21 (m, 1H), 4.11 (dd,  $J = 13.8, 4.8$  Hz, 1H), 4.03 – 3.96 (m, 1H), 3.91 – 3.60 (m, 6H), 3.60 – 3.32 (m, 2H), 3.15 (s, 1H), 2.18 (s,



1H), 1.65 - 1.53 (m, 4H), 1.25 (s, 46H), 0.88 (t,  $J = 6.5$  Hz, 6H).

**Synthesis of 6-O-benzyl-4-hydroxy-2,3-O-tetradecane- $\alpha$ -ethanethiol-D-glucopyranose (20)**



Compound (**20**) was synthesized from (**18**, 100 mg, 0.1418 mmol) using the general procedure 2 above (yield, 85.23 mg, 85%).

(**20**):  $^1H$  NMR (300 MHz, Chloroform-*d*)  $\delta$  7.36 - 7.27 (m, 5H), 4.57 (s, 2H), 4.37 (d,  $J = 9.6$  Hz, 1H), 3.92 - 3.57 (m, 8H), 3.52 - 3.40 (m, 2H), 3.23 (t,  $J = 8.6$  Hz, 1H), 3.08 (t,  $J = 9.2$  Hz, 1H), 2.74 - 2.68 (m, 2H), 1.64 - 1.56 (m, 6H), 1.33 - 1.24 (m, 44H), 0.88 (t,  $J = 6.5$  Hz, 6H).

**Preparation of compounds for cellular treatment**

Lipid A derivatives were placed under hi-vacuum and weighed by difference using an analytical balance in solid form. Then, an appropriate volume of DMSO was added to the compounds to give a concentrated working stock solution for cellular treatment. The stock solution was serial diluted with DMSO to

afford the desired concentration range. The final DMSO concentration was maintained at 0.5%.

### **LPS antagonistic activity assay and cell culture**

Human THP-1 cells that were in 1 mL aliquots and were stored in liquid nitrogen (Cane 4-level 1), were thawed and diluted 1:10 in fresh growth medium and cultured in a T-75 flask. THP-1 growth medium was RPMI 1640 containing 10% FBS, 50 U/mL penicillin, 50 µg/mL streptomycin, 50µM β-mercapto-ethanol. THP-1 assay medium was the same as growth medium but with only 2% FBS. For cellular assays, THP-1 monocytes were centrifuged and resuspended to a cell concentration of  $1 \times 10^6$  cells/mL. LPS dilutions were conducted from 1 mg/mL UP LPS Invivogen Stock to achieve desired final concentration (see plate arrangement below). 96-well plate was then treated as follows: (1) Added 5µl of the LPS to some wells and added sterile water to the control wells, with 3 replicates for each concentration and 0.5% DMSO was used for control i.e. A (DMSO only) is added to wells A1, A2, and A3 triplicates with LPS and A4, A5, & A6 triplicates without LPS and so forth, (2) cells were incubated at 37°C for 6 hours. After 6 hours, the entire solution from each well was removed, centrifuged for 10 mins to remove cells and the supernatant was placed in

Eppendorf tubes and frozen at -20°C, (3) conducted ELISA to analyze secreted TNF $\alpha$  production.

Plate arrangement:

<b>Final conc. <math>\mu</math>M</b>	<b>LPS</b>	<b>LPS</b>	<b>LPS</b>	<b>-LPS</b>	<b>-LPS</b>	<b>-LPS</b>
0 (DMSO only)	A1	A2	A3	A4	A5	A6
1	B1	B2	B3	B4	B5	B6
3	C1	C2	C3	C4	C5	C6
10	D1	D2	D3	D4	D5	D6
30	E1	E2	E3	E4	E5	E6
100	F1	F2	F3	F4	F5	F6

**TNF $\alpha$  ELISA**

**Reagents:**

**A. TNF $\alpha$  capture antibody:** MAB610 (R&D Systems), 500  $\mu$ g reconstituted in 1 ml PBS, 500  $\mu$ g/ml, aliquots (50  $\mu$ l) stored in -80 °C freezer, diluted to 2  $\mu$ g/ml in PBS for assay.

**B. TNF $\alpha$  detection antibody:** BAF210 (R&D Systems), biotinylated, 50  $\mu$ g reconstituted in 1 ml detection antibody diluent, 50  $\mu$ g/ml, aliquots (50  $\mu$ l) stored in -80 °C freezer, diluted to 0.1  $\mu$ g/ml for assay.

**C. TNF $\alpha$  recombinant protein (for standard curve):** 210-TA (R&D Systems), 10  $\mu$ g reconstituted in 10 ml standard diluent buffer. Stored aliquots at -80 °C after snap-freezing in EtOH/dry ice. Diluted 0.5 ml to 5 ml (100 ng/ml) in standard diluent buffer.

**D. ELISA Buffers:**

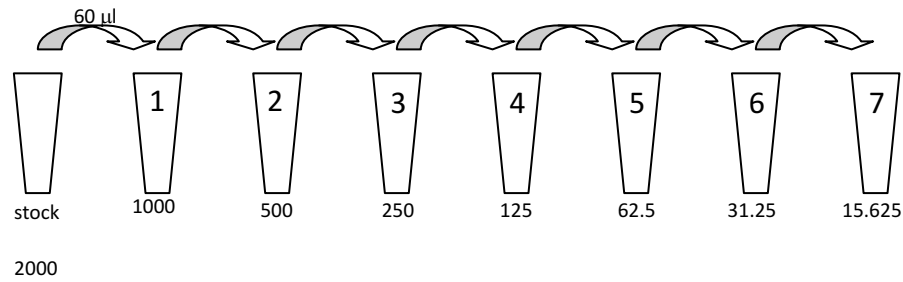
*Wash*; PBS containing 0.05% Tween 20 (5 ml 5% Tween 20, dilute with PBS to 500 ml); *Sample Diluent*, 20 mM Tris, pH 7.3 containing 150 mM NaCl, 0.1% BSA, and 0.05% Tween 20; *Blocking buffer*, PBS containing 1% BSA, 5% sucrose, and 0.05% NaN<sub>3</sub>; *Detection Antibody Diluent*, 20 mM Tris, pH 7.3 containing 150 mM NaCl and 0.1% BSA; *Conjugate Diluent*, PBS containing 1% BSA; *Stop Solution*, 1 M H<sub>2</sub>SO<sub>4</sub>, prepared from 96% stock. Diluted 1:10 to make 1.8 M for assay; *Standard Diluent*, PBS containing 0.1% BSA.

#### **Plate Preparation for ELISA**

Applied 100 µl capture antibody (2 µg/ml) to required wells. Sealed and incubated overnight at room temperature. Then washed x3 with wash buffer and applied 300 µl blocking buffer. Then incubated 1 h at room temperature followed by wash.

#### **ELISA Assay Procedure:**

Standard curve preparation - Diluted refrigerated standard (0.1 µg/ml) to 2000 pg/ml and performed serial dilutions in standard diluent buffer with 60 µl.



Then added 50 µl sample diluent buffer plus 50 µl standards and samples. Used 50 µl H<sub>2</sub>O for 0 pg/ml standard and mixed by gently tapping plate. Then sealed and incubated at room temperature for 2 h. Then washed 3x with wash buffer and added 100 µl biotinylated detection antibody (0.1 µg/ml) and sealed and incubated for 2 h at room temperature. Then washed 3x with wash buffer and added 100 µl streptavidin HRP with 1/200 dilution into conjugate diluent, sealed and incubated for 20 min at room temperature. Then washed 3x with wash buffer and prepared substrate solution by mixing equal volumes of color reagent A & B within 15 minutes of use. Then added 100 µl of substrate solution to each well and incubated for 30 minutes. Then added 50 µl stop solution and mixed by gently tapping. Then covered and read wells with absorbance plate reader at 450 nm and at 630 nm to subtract out optical differences between wells.

## VI. References

1. Madigan, M. T., Martinko, J. M., Bender, K. S., Buckley, D. H. & Stahl, D. A. *Brock biology of microorganisms*. (2014).
2. Pappaterra Mendoza, G. J. *et al.* In Vitro and In Vivo Effects of an Immunomodulator Composed of Escherichia Coli Lipopolysaccharide and Propionibacterium granulosum-Inactivated Cells in Pigs. *J. Vet. Med. Ser. B* **47**, 619–627 (2000).
3. Nduka, O. O. & Parrillo, J. E. The Pathophysiology of Septic Shock. *Sepsis* **23**, 41–66 (2011).
4. Novosad, S. & Sapiano, M. Epidemiology of Sepsis: Prevalence of Health Care Factors and Opportunities for Prevention. *Morb. Mortal. Wkly. Rep. MMWR* **65**, 864–869 (2016).
5. Motzkus, C. A. *et al.* ICU Admission Source as a Predictor of Mortality for Patients With Sepsis. *J. Intensive Care Med.* 885066617701904 (2017).  
doi:10.1177/0885066617701904
6. Torio, C. & Moore, B. National Inpatient Hospital Costs: The Most Expensive Conditions by Payer, 2013. (2016).
7. GINSBURG, I. The role of bacteriolysis in the pathophysiology of inflammation, infection and post-infectious sequelae. *APMIS* **110**, 753–770 (2002).

8. Penack, O. *et al.* Management of sepsis in neutropenic patients: 2014 updated guidelines from the Infectious Diseases Working Party of the German Society of Hematology and Medical Oncology (AGIHO). *Ann. Hematol.* **93**, 1083–1095 (2014).
9. Schaffzin, D. M. & Wong, W. D. Nonoperative Management of Complicated Diverticular Disease. *Clin. Colon Rectal Surg.* **17**, 169–176 (2004).
10. Annane, D. *et al.* Corticosteroids for severe sepsis and septic shock: a systematic review and meta-analysis. *BMJ* **329**, 480 (2004).
11. Salluh, J. I. F. & Póvoa, P. Corticosteroids in Severe Sepsis and Septic Shock: A Concise Review. *Shock* **47**, (2017).
12. Canady, J., Williams, W., Thompson, I., Vincent, G. S. & Hoover, E. Use of naloxone in septic shock. *J. Natl. Med. Assoc.* **81**, 669–673 (1989).
13. Oettinger, C. W. & D'Souza, M. J. Microencapsulated drug delivery: a new approach to pro-inflammatory cytokine inhibition. *J. Microencapsul.* **29**, 455–462 (2012).
14. Werdan, K. Pathophysiology of Septic Shock and Multiple Organ Dysfunction Syndrome and Various Therapeutic Approaches with Special Emphasis on Immunoglobulins. *Ther. Apher.* **5**, 115 (2001).
15. WESTPHAL, O. & LUDERITZ, O. Chemical and biological analysis of highly purified bacterial polysaccharides. *Dtsch Med Wochenschr* **78**, 9–17 (1953).
16. Christie, W. Lipid A and bacterial lipopolysaccharides: structure, occurrence and biology. *lipidlibrary.aocs.org* (2014). Available at: <http://lipidlibrary.aocs.org/Primer/content.cfm?ItemNumber=39339>.

17. Heinrichs, D. E., Yethon, J. A. & Whitfield, C. Molecular basis for structural diversity in the core regions of the lipopolysaccharides of *Escherichia coli* and *Salmonella enterica*. *Mol. Microbiol.* **30**, 221–232 (1998).
18. Tacken, A., Rietschel, E. T. & Brade, H. Methylation analysis of the heptose/3-deoxy-d-manno-2-octulosonic acid region (inner core) of the lipopolysaccharide from *Salmonella minnesota* rough mutants. *Carbohydr. Res.* **149**, 279–291 (1986).
19. Sadovskaya, I. *et al.* Structural characterization of the outer core and the O-chain linkage region of lipopolysaccharide from *Pseudomonas aeruginosa* serotype O5. *Eur. J. Biochem.* **267**, 1640–1650 (2000).
20. Lerouge, I. & Vanderleyden, J. O-antigen structural variation: mechanisms and possible roles in animal/plant–microbe interactions. *FEMS Microbiol. Rev.* **26**, 17–47 (2002).
21. White, A. F. B. & Demchenko, A. V. Chapter 5 - Modulating LPS Signal Transduction at the LPS Receptor Complex with Synthetic Lipid A Analogues. in *Advances in Carbohydrate Chemistry and Biochemistry* (ed. Derek Horton) **Volume 71**, 339–389 (Academic Press, 2014).
22. Wang, X. & Quinn, P. J. Lipopolysaccharide: Biosynthetic pathway and structure modification. *Prog. Lipid Res.* **49**, 97–107 (2010).
23. Molinaro, A. *et al.* Chemistry of Lipid A: At the Heart of Innate Immunity. *Chem. – Eur. J.* **21**, 500–519 (2015).
24. Parham, P. *The Immune System*. (Garland Science, 2014).



25. Kitchens, R. L. & Thompson, P. A. Modulatory effects of sCD14 and LBP on LPS-host cell interactions. *J. Endotoxin Res.* **11**, 225–229 (2005).
26. Park, B. S. & Lee, J.-O. Recognition of lipopolysaccharide pattern by TLR4 complexes. *Exp Mol Med* **45**, e66 (2013).
27. Beamer, L. J., Carroll, S. F. & Eisenberg, D. The BPI/LBP family of proteins: a structural analysis of conserved regions. *Protein Sci. Publ. Protein Soc.* **7**, 906–914 (1998).
28. Pugin, J. CD14 is a pattern recognition receptor. *Immunity* **1**, 509–516 (1994).
29. Devitt, A. Human CD14 mediates recognition and phagocytosis of apoptotic cells. *Nature* **392**, 505–509 (1998).
30. Lu, Y.-C., Yeh, W.-C. & Ohashi, P. S. LPS/TLR4 signal transduction pathway. *Cytokine* **42**, 145–151 (2008).
31. Landmann, R. Increased circulating soluble CD14 is associated with high mortality in Gram-negative septic shock. *J Infect Dis* **171**, 639–644 (1995).
32. Leturcq, D. J. Antibodies against CD14 protect primates from endotoxin-induced shock. *J Clin Invest* **98**, 1533–1538 (1996).
33. Yu, B., Hailman, E. & Wright, S. D. Lipopolysaccharide binding protein and soluble CD14 catalyze exchange of phospholipids. *J Clin Invest* **99**, 315–324 (1997).
34. Wright, S. D., Ramos, R. A., Tobias, P. S., Ulevitch, R. J. & Mathison, J. C. CD14, a receptor for complexes of lipopolysaccharide (LPS) and LPS binding protein. *Science* **249**, 1431–1433 (1990).

35. Werner, T. A family of peptidoglycan recognition proteins in the fruit fly *Drosophila melanogaster*. *Proc Natl Acad Sci USA* **97**, 13772–13777 (2000).
36. Vasselon, T. & Detmers, P. A. Toll receptors: a central element in innate immune responses. *Infect Immun* **70**, 1033–1033 (2002).
37. Park, B. S. *et al.* The structural basis of lipopolysaccharide recognition by the TLR4–MD-2 complex. *Nature* **458**, 1191–1195 (2009).
38. Shimazu, R. MD-2, a molecule that confers lipopolysaccharide responsiveness on Toll-like receptor 4. *J Exp Med* **189**, 1777–1782 (1999).
39. Liu, S. F. & Malik, A. B. NF- $\kappa$ B activation as a pathological mechanism of septic shock and inflammation. *Am. J. Physiol. - Lung Cell. Mol. Physiol.* **290**, L622 (2006).
40. Brieger, A., Rink, L. & Haase, H. Differential Regulation of TLR-Dependent MyD88 and TRIF Signaling Pathways by Free Zinc Ions. *J. Immunol.* **191**, 1808 (2013).
41. Dinarello, C. A. Proinflammatory and anti-inflammatory cytokines as mediators in the pathogenesis of septic shock. *Chest* **112**, 321S–329S (1997).
42. Cabal-Hierro, L. & Lazo, P. S. Signal transduction by tumor necrosis factor receptors. *Cell. Signal.* **24**, 1297–1305 (2012).
43. da Silva, A. M. T. *et al.* Shock and Multiple-Organ Dysfunction after Self-Administration of Salmonella Endotoxin. *N. Engl. J. Med.* **328**, 1457–1460 (1993).
44. Pfeffer, K. Biological functions of tumor necrosis factor cytokines and their receptors. *TNF Superfamily* **14**, 185–191 (2003).
45. van der Poll, T. *et al.* Activation of Coagulation after Administration of Tumor Necrosis Factor to Normal Subjects. *N. Engl. J. Med.* **322**, 1622–1627 (1990).

46. Aderka, D. Role of tumor necrosis factor in the pathogenesis of intravascular coagulopathy of sepsis: potential new therapeutic implications. *Isr. J. Med. Sci.* **27**, 52–60 (1991).
47. Kotani, S. *et al.* Immunobiologically active lipid A analogs synthesized according to a revised structural model of natural lipid A. *Infect. Immun.* **45**, 293–296 (1984).
48. Bowen, W. S., Gandhapudi, S. K., Kolb, J. P. & Mitchell, T. C. Immunopharmacology of Lipid A Mimetics. *Immunopharmacology* **66**, 81–128 (2013).
49. Opal SM, Laterre P, Francois B & et al. Effect of eritoran, an antagonist of md2-tlr4, on mortality in patients with severe sepsis: The access randomized trial. *JAMA* **309**, 1154–1162 (2013).
50. Shirey, K. A. *et al.* The TLR4 antagonist Eritoran protects mice from lethal influenza infection. *Nature* **497**, 498–502 (2013).
51. Casella, C. R. & Mitchell, T. C. Putting endotoxin to work for us: monophosphoryl lipid A as a safe and effective vaccine adjuvant. *Cell. Mol. Life Sci. CMLS* **65**, 3231–3240 (2008).
52. Cighetti, R. *et al.* Modulation of CD14 and TLR4.MD-2 activities by a synthetic lipid A mimetic. *Chembiochem Eur. J. Chem. Biol.* **15**, 250–258 (2014).
53. Khalaf, J. K. *et al.* Characterization of TRIF Selectivity in the AGP Class of Lipid A Mimetics: Role of Secondary Lipid Chains. *Bioorg. Med. Chem. Lett.* **25**, 547–553 (2015).

54. Matsuura, M., Kiso, M. & Hasegawa, A. Activity of Monosaccharide Lipid A Analogues in Human Monocytic Cells as Agonists or Antagonists of Bacterial Lipopolysaccharide. *Infect. Immun.* **67**, 6286–6292 (1999).
55. Inagawa, H. *et al.* Anti-tumor effect of lipopolysaccharide by intradermal administration as a novel drug delivery system. *Anticancer Res* **17**, (1997).
56. D'Agostini, C. *et al.* Antitumour effect of OM-174 and cyclophosphamide on murine B16 melanoma in different experimental conditions. *Int Immunopharmacol* **5**, (2005).
57. Garay, R. P. *et al.* Cancer relapse under chemotherapy: why TLR2/4 receptor agonists can help. *Eur J Pharmacol* **563**, (2007).
58. Kiani, A. *et al.* Downregulation of the proinflammatory cytokine response to endotoxin by pretreatment with the nontoxic lipid A analog SDZ MRL 953 in cancer patients. *Blood* **90**, (1997).
59. Jeannin, J. F. & Onier, N. Lagadec P, von JN, Stutz P, Liehl E: Antitumor effect of synthetic derivatives of lipid A in an experimental model of colon cancer in the rat. *Gastroenterology* **101**, (1991).
60. Reisser, D., Pance, A. & Jeannin, J. F. Mechanisms of the antitumoral effect of lipid A. *Bioessays* **24**, (2002).
61. Vosika, G. J., Barr, C. & Gilbertson, D. Phase-I study of intravenous modified lipid A. *Cancer Immunol Immunother* **18**, (1984).

62. Isambert, N. *et al.* Phase I study of OM-174, a lipid A analogue, with assessment of immunological response, in patients with refractory solid tumors. *BMC Cancer* **13**, 172 (2013).
63. de Bono, J. S. *et al.* Phase I study of ONO-4007, a synthetic analogue of the lipid A moiety of bacterial lipopolysaccharide. *Clin Cancer Res* **6**, (2000).
64. Engelhardt, R., Mackensen, A. & Galanos, C. Phase I trial of intravenously administered endotoxin (*Salmonella abortus equi*) in cancer patients. *Cancer Res* **51**, (1991).
65. Evans, C., Dalgleish, A. G. & Kumar, D. Review article: immune suppression and colorectal cancer. *Aliment Pharmacol Ther* **24**, (2006).
66. Meng, J., Gong, M., Björkbacka, H. & Golenbock, D. T. Genome-Wide Expression Profiling and Mutagenesis Studies Reveal that Lipopolysaccharide Responsiveness Appears To Be Absolutely Dependent on TLR4 and MD-2 Expression and Is Dependent upon Intermolecular Ionic Interactions. *J. Immunol.* **187**, 3683 (2011).
67. Voet, D. & Voet, J. *Fundamentals of Biochemistry: Life at the Molecular Level.* (Wiley and Sons, 2015).
68. Hilderbrand, R. *The Role of phosphonates in living systems.* (CRC Press, 1983).
69. Engel, R. Phosphonates as analogues of natural phosphates. *Chem. Rev.* **77**, 349–367 (1977).
70. Pompliano, D. L. *et al.* Steady-state kinetic mechanism of ras farnesyl:protein transferase. *Biochemistry (Mosc.)* **31**, 3800–3807 (1992).

71. Bandyopadhyay, S., Dutta, S., Spilling, C. D., Dupureur, C. M. & Rath, N. P. Synthesis and Biological Evaluation of a Phosphonate Analog of the Natural Acetyl Cholinesterase Inhibitor Cyclophostin. *J. Org. Chem.* **73**, 8386–8391 (2008).
72. Magnin, D. R. *et al.*  $\alpha$ -Phosphonosulfonic Acids: Potent and Selective Inhibitors of Squalene Synthase. *J. Med. Chem.* **39**, 657–660 (1996).
73. Zapata, A. J., Gu, Y. & Hammond, G. B. The First  $\alpha$ -Fluoroallenylphosphonate, the Synthesis of Conjugated Fluoroenynes, and the Stereoselective Synthesis of Vinylfluorophosphonates Using a New Multifunctional Fluorine-Containing Building Block. *J. Org. Chem.* **65**, 227–234 (2000).
74. Bartlett, P. A. & Giangordano, M. A. Transition State Analogy of Phosphonic Acid Peptide Inhibitors of Pepsin. *J. Org. Chem.* **61**, 3433–3438 (1996).
75. Dappen, M. S. *et al.* Synthesis and biological evaluation of cyclopropyl analogs of 2-amino-5-phosphonopentanoic acid. *J. Med. Chem.* **34**, 161–168 (1991).
76. Walker, D. M., McDonald, J. F., Franz, J. E. & Logusch, E. W. Design and synthesis of [ $\gamma$ ]-oxygenated phosphinothricins as inhibitors of glutamine synthetase. *J. Chem. Soc. [Perkin 1]* 659–666 (1990). doi:10.1039/P19900000659
77. Sikorski, J. A. *et al.* EPSP Synthase: The Design and Synthesis of Bisubstrate Inhibitors Incorporating Novel 3-Phosphate Mimics. *Phosphorus Sulfur Silicon Relat. Elem.* **76**, 115–118 (1993).
78. Glabe, A. R., Sturgeon, K. L., Ghizzoni, S. B., Musker, W. K. & Takahashi, J. N. Novel Functionalized Acylphosphonates as Phosphonoformate Analogs. *J. Org. Chem.* **61**, 7212–7216 (1996).

79. Atherton, F. R., Hali, M. J., Hassall, C. H., Lambert, R. W. & Ringrose, P. S. Phosphonopeptides as Antibacterial Agents: Rationale, Chemistry, and Structure-Activity Relationships. *Antimicrob. Agents Chemother.* **15**, 677–683 (1979).
80. Kim, C. U., Luh, B. Y. & Martin, J. C. Regiospecific and highly stereoselective electrophilic addition to furanoid glycols: synthesis of phosphonate nucleotide analogs with potent activity against HIV. *J. Org. Chem.* **56**, 2642–2647 (1991).
81. Rijkers, D. S., Wielders, S. J. H., Tesser, G. I. & Hemker, H. C. Design and synthesis of thrombin substrates with modified kinetic parameters. *Thromb. Res.* **79**, 491–499
82. Dixon, H. B. F. & Sparkes, M. J. Phosphonomethyl analogues of phosphate ester glycolytic intermediates. *Biochem. J.* **141**, 715–719 (1974).
83. McEldoon, W. L., Lee, K. & Wiemer, D. F. Synthesis of nucleoside  $\alpha$ -hydroxy phosphonates. *Int. J. Rapid Publ. Prelim. Commun. Org. Chem.* **34**, 5843–5846 (1993).
84. Serra, C., Dewynter, G., Montero, J.-L. & Imbach, J.-L. 3'-C-phosphonates as nucleotides analogues synthesis starting from original C-phosphonosugars (in ribo- and deoxyribo- series). *Int. J. Rapid Publ. Crit.* **50**, 8427–8444 (1994).
85. Chen, X., Wiemer, A. J., Hohl, R. J. & Wiemer, D. F. Stereoselective Synthesis of the 5'-Hydroxy-5'-phosphonate Derivatives of Cytidine and Cytosine Arabinoside. *J. Org. Chem.* **67**, 9331–9339 (2002).
86. Nijland, R., Hofland, T. & van Strijp, J. A. G. Recognition of LPS by TLR4: Potential for Anti-Inflammatory Therapies. *Mar. Drugs* **12**, 4260–4273 (2014).

87. Boulineau, F. P. & Wei, A. Mirror-Image Carbohydrates: Synthesis of the Unnatural Enantiomer of a Blood Group Trisaccharide. *J. Org. Chem.* **69**, 3391–3399 (2004).
88. Kaeothip, S. *et al.* Development of LPS antagonistic therapeutics: synthesis and evaluation of glucopyranoside-spacer-amino acid motifs. *RSC Adv.* **1**, 83–92 (2011).